Review

Mechanism of the calcium-regulation of muscle contraction —In pursuit of its structural basis—

By Takeyuki WAKABAYASHI[*1,*2,†]

(Communicated by Masanori OTSUKA, M.J.A.)

Abstract: The author reviewed the research that led to establish the structural basis for the mechanism of the calcium-regulation of the contraction of striated muscles. The target of calcium ions is troponin on the thin filaments, of which the main component is the double-stranded helix of actin. A model of thin filament was generated by adding tropomyosin and troponin. During the process to provide the structural evidence for the model, the troponin arm was found to protrude from the calcium-depleted troponin and binds to the carboxyl-terminal region of actin. As a result, the carboxyl-terminal region of tropomyosin shifts and covers the myosin-binding sites of actin to block the binding of myosin. At higher calcium concentrations, the troponin arm changes its partner from actin to the main body of calcium-loaded troponin. Then, tropomyosin shifts back to the position near the grooves of actin double helix, and the myosin-binding sites of actin becomes available to myosin resulting in force generation through actin-myosin interactions.

Keywords: striated muscle, calcium-regulation, actin, tropomyosin, troponin, cardiomyopathy

Introduction

Actin was first isolated from rabbit skeletal muscle as a protein factor to activate the myosin ATPase by about 100-fold.[1),2)] Soon after its discovery, it was found that a monomeric globular actin (G-actin) with the molecular mass of 42 kDa contains one ATP and that the polymerization of monomeric actin (globular actin, G-actin) to form filaments (filamentous actin, F-actin) is dependent on Mg^{2+} and KCl, and facilitates the hydrolysis of ATP. The ATP-hydrolysis is required for the treadmilling[3)] of actin filaments, where the dynamic cycle of polymerization and depolymerization of actin takes place, while the length of the actin filaments is maintained nearly constant with some length fluctuation at both ends.[4)]

In muscle cells, the stability of the polymerized sarcomeric actin (F-actin) is important to interact with myosin to generate force. The dynamic cycle of the polymerization and depolymerization of cytoplasmic actin is required for many other cell functions such as cell adhesion, cellular signaling, intracellular trafficking, cell division, and synaptic functions.[5)]

Both of sarcomeric and cytoplasmic actin filaments are usually associated with tropomyosin. *Tetrahymena* actin, which cannot bind rabbit skeletal tropomyosin, is a rare exception.[6)] A tropomyosin molecule is thought to be a canonical coiled-coil protein, about 40 nm in length, which binds to actin filament covering seven contiguous actin protomers (monomers),[7)] with the length of an actin protomer being about 5.5 nm.

[*1] Department of Physics, Graduate School of Science, the University of Tokyo, Tokyo, Japan.

[*2] Department of Biosciences, Graduate School of Science and Engineering, Teikyo University, Tochigi, Japan.

[†] Correspondence should be addressed: T. Wakabayashi, Department of Biosciences, Graduate School of Science and Engineering, Teikyo University, 1-1 Toyosatodai, Utsunomiya 320-8551, Japan (e-mail: tw007@nasu.bio.teikyo-u.ac.jp; tkyk.wakabayashi@gmail.com).

Abbreviations: ADP: adenosine diphosphate; AMPPNP: β,γ-imidoadenosine 5′-triphosphate; ATP: adenosine triphosphate; BFP: blue fluorescent protein; COOH-terminal: carboxyl-terminal; C-domain: carboxyl terminal domain; EGTA: ethylene glycol tetraacetic acid; GFP: green fluorescent protein; N-domain: amino-terminal domain; NH-terminal: amino-terminal; Pi: inorganic phosphate; S1: subfragment 1 of myosin; TnC: troponin-C; TnI: troponin-I; TnT: troponin-T; TnT_1: troponin-T_1; TnT_2: troponin-T_2; Tn-(I+C): binary complex of TnI and TnC; Tn-(T_2+I+C): ternary complex of TnT_2, TnI, and TnC; Vi: vanadate.

doi: 10.2183/pjab.91.321

In skeletal or cardiac muscles, actin filaments are also associated with troponin,[8] which is a calcium-binding protein that regulates contraction. Troponin consists of three components or subunits,[9),10] tropomyosin-binding subunit (Tn-T),[11] inhibitory subunit (Tn-I),[12] and calcium-binding subunit (Tn-C).[13] Both of troponin and tropomyosin are essential for the calcium-regulation of striated muscle. Mutations of troponin or tropomyosin cause the familiar cardiac myopathy.

In this review, three major functions of actin-tropomyosin-troponin will be described: (i) The Ca^{2+}-dependent movement of troponin and tropomyosin on actin filament, (ii) the interaction site(s) with myosin, and lastly (iii) the structure of the tropomyosin junction, of which the formation is essential to bind to actin filaments.

1. Structures of actin-containing filaments

1.1. F-actin model. Figure 1A shows the model for the double-stranded structure of the actin filaments proposed by Hanson and Lowy[14] on the basis of electron microscopy. The double strands are right-handed.[15] The distance between the crossovers of the two strands, indicated by arrows in Fig. 1 is 36 nm. Each sphere represents an actin monomer, which is strictly speaking a protomer of actin filaments, with the diameter of 5.5 nm. There are 13 monomers per crossover. By taking advantage of the helical symmetry of actin filaments,[16] the three-dimensional structures of actin-containing filaments were reconstructed from electron micrographs of negatively stained specimens.[17] However, the polarity of the filaments was not clear.

1.2. Models of actin-tropomyosin-troponin. Troponin and tropomyosin are indispensable for the physiological regulation of striated muscle contraction.[18] The reason why troponin is essential is straightforward to understand, because it binds calcium ions[19] and changes its structure with Ca^{2+}.[20] However, the role of tropomyosin was obscure.

Figures 1B–C show the thin-filament models put forward by the Ebashi group[21)–25] to explain the role of tropomyosin and to account for the large gaps (~40 nm) between troponin molecules.[26] In these models, the Ca^{2+}-induced change takes place in one troponin molecule can be transferred to one tropomyosin molecule, which in turn spreads the change to several actin molecules covered by one tropomyosin. By analyzing electron micrographs of actin-tropomyosin-troponin with a homemade optical diffractometer, the stoichiometry of actin and troponin was

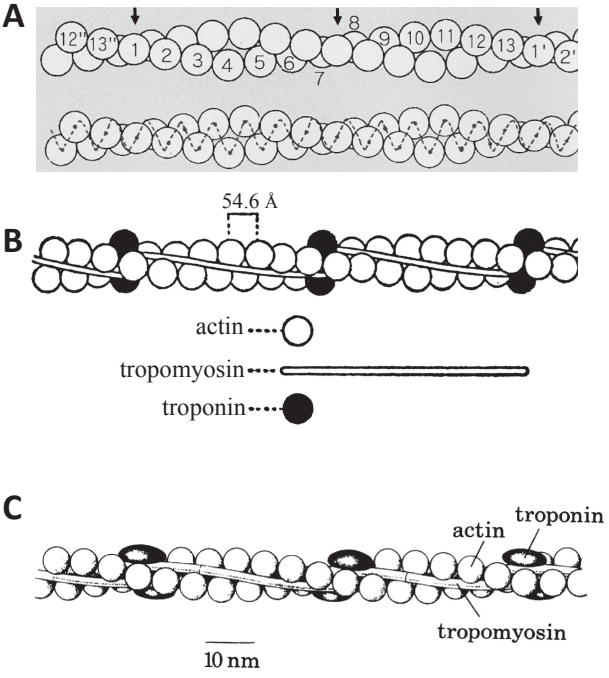

Fig. 1. Models of thin filament from striated muscles. A. Helical arrangement of the globular protomers (monomers) in an actin filament.[14] The protomers are drawn as spheres. The centers of the protomers are helically arranged as shown in the lower panel, in which a short-pitched left-handed helix is drawn in a dotted line. The crossover points of the long-pitched right-handed double helix are indicated by arrows. There are 13 protomers (monomers) per crossover. B–C. The models of actin-tropomyosin-troponin proposed by the Ebashi group.[21)–25] In the initial model (B),[21),23] troponin was drawn as a sphere for simplicity. In the model refined by Ohtsuki (C), the spatial relationship between the end of tropomyosin molecule and the troponin-binding site of tropomyosin was incorporated, and the relative positions of troponin molecules on the opposite sides of actin double helix were assumed to follow the helical symmetry of actin and stagger by 27.3 Å.[24),25] The 27.3 Å staggering of troponin was shown experimentally,[84] and its detail is described in the section 4.

determined to be exactly seven to one.[7] This is consistent with the biochemical data.[27] Since the stoichiometry of tropomyosin and troponin is one to one,[28] this means that one tropomyosin binds seven actin monomers. This number is consistent with the 14-fold (7 × 2) periodicity of the amino acid sequence of tropomyosin.[29]

These thin-filament models can also explain the changes in the X-ray diffraction pattern upon the contraction of living frog muscle. Because tropomyosin molecules lie near the two grooves of actin double strands, the whole thin filaments can be approximated by four strands at low resolution. In such a situation, the intensity of the second actin layer-line

should be strong. However, it should become weaker, when tropomyosin dislocates from the grooves of actin strands. Indeed, the second layer-line became weaker in a relaxed state.[30)–32)] By analyzing the X-ray diffraction patterns from relaxed and contracting muscles, it was proposed that the tropomyosin dislocates from the actin grooves in a relaxed state and would block the myosin binding to actin filaments. This hypothesis proposed that the actin-myosin interaction is blocked sterically by shifted tropomyosin. However, a crucial question remained to be answered, that is, whether the shifted tropomyosin actually covers the myosin-binding site(s) on actin. The answer to the question is described in the section 4.4.

More direct evidence for the shift of tropomyosin also was required, because the positions of tropomyosin were deduced indirectly from the intensities of actin layer-lines. To provide the evidence, three-dimensional structures of actin-containing filaments had been reconstructed using helical symmetry.[17),33)] However, the change in the spatial relationship between actin and tropomyosin was not established.

1.3. Structural changes in the three-dimensional structures of actin-tropomyosin-troponin. Figure 2 shows the first direct evidence for the change in the positions of tropomyosin relative to actin: The three-dimensional structure of actin-tropomyosin complex representing an active state was different from that of actin-tropomyosin-TnT-TnI complex, which represents a relax state.[34)] Both of the structures were reconstructed from electron micrographs of negatively stained specimens assuming the helical symmetry of actin filaments. In a relaxed state (Fig. 2C), tropomyosin is dislocated from the actin grooves and associated more intimately with actin than in an active state (Fig. 2D). This is consistent with the results obtained by quasi-elastic scattering of actin-tropomyosin-troponin filaments: The bending motion of filaments was suppressed at low Ca^{2+} concentrations.[35)]

The three-dimensional structures provided the more direct evidence for the steric blocking mechanism, and explain the decrease in the intensity of the second actin layer-line and the increase in the third one of X-ray diffraction pattern upon muscle relaxation. However, to prove the steric blocking mechanism, it was essential to show that the dislocated tropomyosin actually blocks the myosin-binding site(s) of actin filaments. It took us more than a quarter of a century to obtain this structural information as described in the sections 2 and 4.

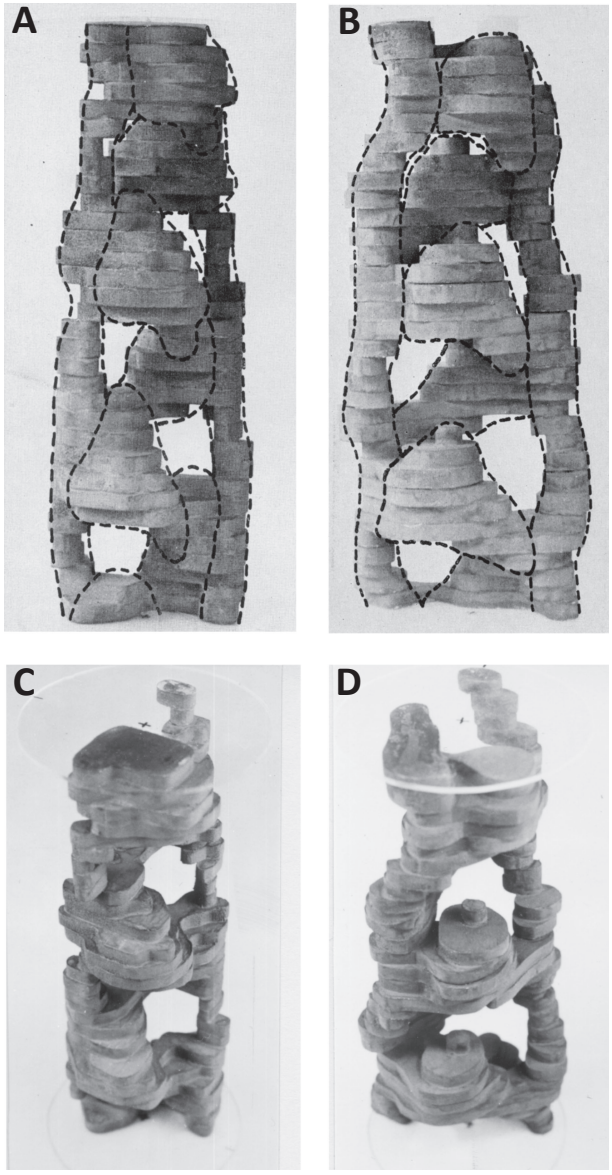

Fig. 2. Solid models of actin-containing filament reconstructed from electron micrographs of negatively stained filaments by assuming the helical symmetry of specimens.[34)] A. A front view of a solid model of the complex of actin, tropomyosin, troponin-T, and troponin-I. It represents an inhibited state of thin filaments. B. A front view of actin-tropomyosin representing an active state of thin filament. C. An oblique view of the model shown in A (inhibited state). D. An oblique view of the model shown in B (active state). In an inhibited state, actin and tropomyosin associate more firmly.

Figure 2 also shows the conspicuous polarity of the actin-containing filaments for the first time. The actin protomer (monomer) appeared to be triangular in profile, with one end being convex and the other concave. The polar nature of actin protomer became

clearer by applying a new method to average several three-dimensional structures.[34),36)] However, the direction of the convex surface of actin in sarcomeres could not be determined at this time.

The complex of actin filaments with myosin shows a polar structure called an arrowhead pattern,[37)] which points away from the Z-band of sarcomere. To solve the problem of polarity in sarcomere and to determine the myosin-binding site(s) of actin filaments, better electron micrographs were collected by applying minimal electron dose procedures to reduce the deformation of the specimens due to radiation damage.

2. Determination of actin-myosin interface

2.1. Polarity of actin filament. At the growing edge of the developing axons of neurons, actin filaments elongate to push the cell membrane, but at the other end actin monomers detach from the filaments. The combination of polymerization at the elongating plus-end and depolymerization at the minus-end is called treadmilling, which is proposed to play important roles in cytokinesis of amoeboid cells.[3)] Therefore, the structure of actin filaments should have polarity. The first evidence for the polar nature of actin filament was the arrowhead pattern revealed by adding myosin heads to actin filaments.[37)] The arrowheads point away from the Z-band of sarcomere. The polar structure of actin filament itself without decorating with myosin was provided by three-dimensional image reconstruction from electron micrographs.[34)] In the reconstructed image, an actin protomer (monomer) appears to be a cone. However, whether the apex of the cone points the Z-band or M-line could not be determined. Therefore, the polarity of actin filaments was determined by comparing the structures of actin filaments and that with myosin subfragment-1 (S1), and it was concluded that the cone-shaped actin protomer points towards Z-band as will be described in the section 2.3.

2.2. Structure of the complex of actin filament and myosin. By chymotryptic digestion, myosin can be divided into heads and a tail. The head, called myosin subfragment-1 (S1), contains two important functional sites to bind to actin filaments and to bind ATP. The head part of myosin represents the ATP-hydrolyzing enzymatic activity of the whole myosin. Its ATPase activity is activated 100-fold through the interaction with actin filaments and this actin-myosin interaction generates force. In the absence of Mg^{2+}-ATP, myosin S1 strongly binds to actin filaments to form the so-called rigor complex, which shows the arrowhead pattern.

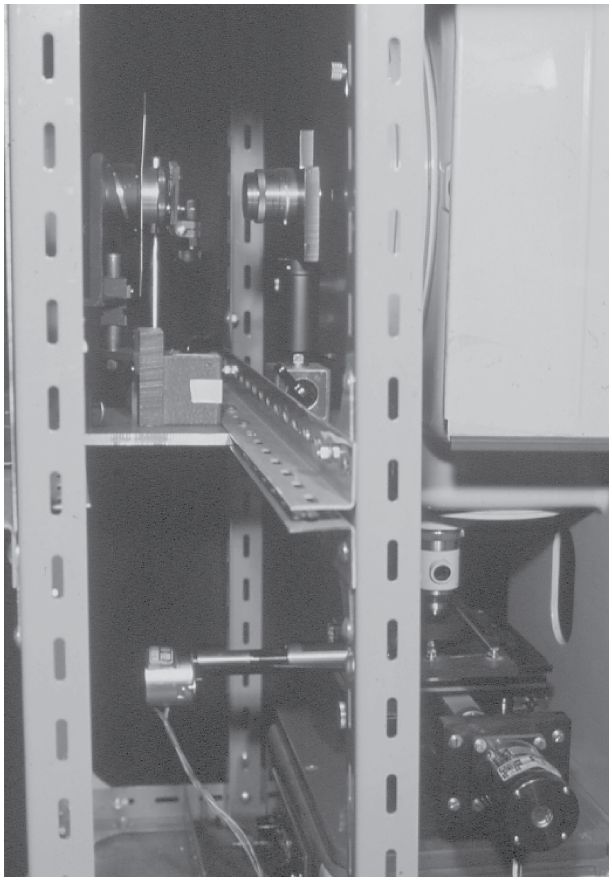

Fig. 3. A homemade computer-controlled microdensitometer constructed to digitize electron micrographs. The two-dimensional stage was driven using two stepping motors controlled by a mini-computer, and the optical path of a Nikon shadowgraph was reversed to illuminate only the small area to minimize the Schwarzschild-Villiger effect.[38)] The lamp was driven by a stabilized direct-current power source for constant illumination.

The electron micrographs have to be digitized for data processing to reconstruct three-dimensional images. Figure 3 shows a homemade computer-controlled microdensitometer (T. Wakabayashi and K. Nagasawa, unpublished work). The two-dimensional stage of a Nikon shadowgraph was driven using two stepping motors controlled by a mini-computer, and the optical path was reversed to illuminate only the small area to minimize the Schwarzschild-Villiger effect.[38)]

Figure 4A shows the three-dimensional structure of the complex of the actin-tropomyosin and myosin S1.[39)] By examining the arrowhead pattern of the original electron micrographs, the polarity of

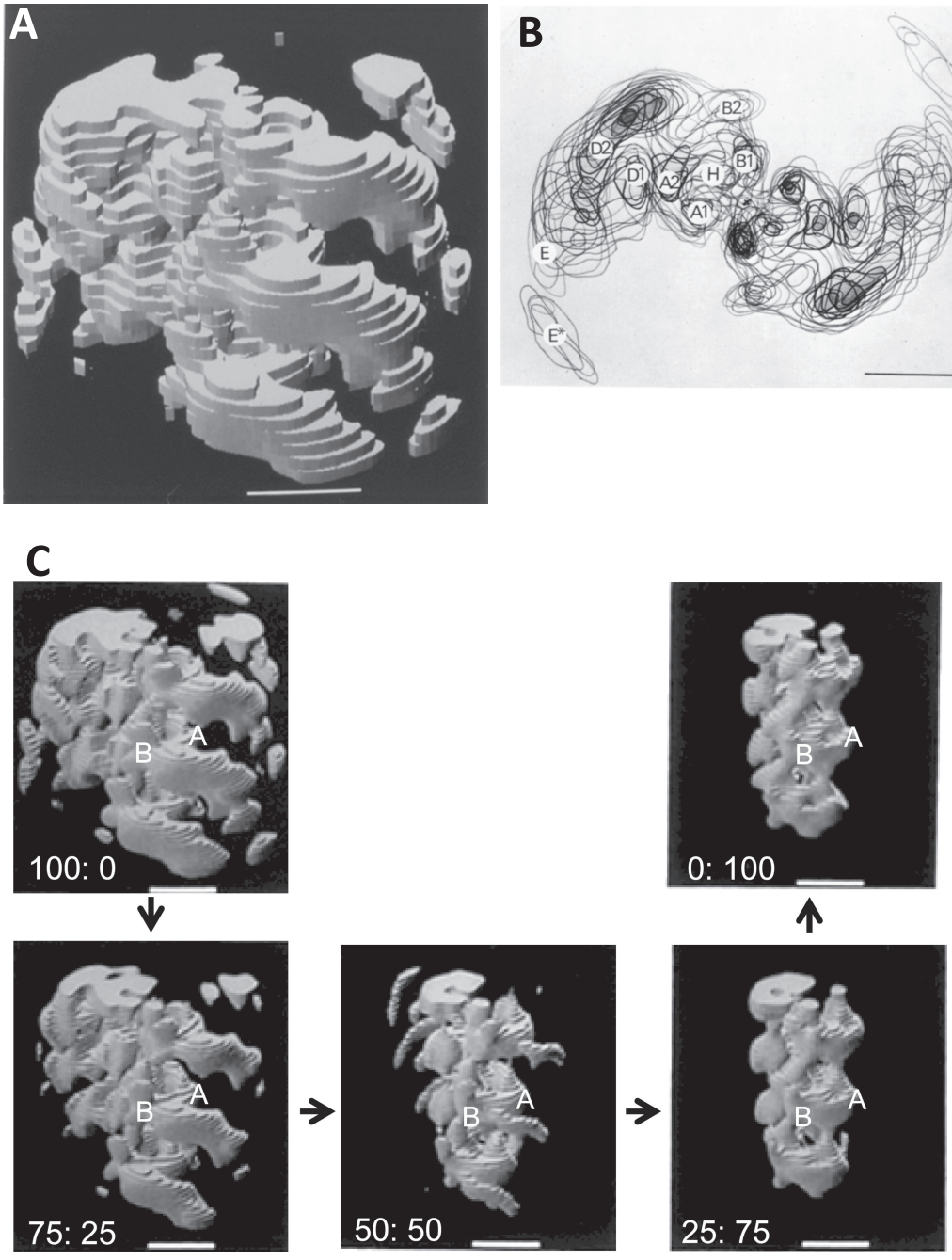

Fig. 4. The three-dimensional structure of the actin-tropomyosin-myosin S1 complex reconstructed from electron micrographs of negatively stained complexes by assuming the helical symmetry of specimens.[39] A. The oblique view from the M-line side. B. The top view of the superposed two-dimensional sections showing the multi-domain structure.[41] C. The visual validation of the objective assignment of actin. The top two panels show the actin-tropomyosin-myosin S1 complex on the left, and the actin-tropomyosin complex without myosin S1 on the right. The weighted averages of two structures with various weighting factors were calculated and are shown in the bottom three panels. It was concluded that both of domains A and B correspond to actin-tropomyosin and that the domains A2 and B2 represent the myosin-binding site of actin.

the actin in Fig. 4C could be determined: The solid model shown in Fig. 4A is viewed obliquely from the M-line side.[39] This means that the concave surface of the actin monomer is nearer to the M-line and that the solid models shown in Figs. 2C–D were viewed from the Z-band side. Therefore, the models in Figs. 2C–D were inverted to compare with that shown in Fig. 4A. This polarity is consistent with that concluded by Taylor and Amos.[40]

Figure 4B shows the top view of the superposed two-dimensional sections. The actin-tropomyosin-myosin S1 complex shows the multi-domain structure.[41] It can be divided into domains A (A1, A2), B (B1, B2), D (D1, D2), E, and E*. Because the diameter of an actin filament is about 8 nm, it was straightforward to assign the domains D2, E, and E* as myosin S1, of which the radius from the axis of helical symmetry are larger than 8 nm.

2.3. Determination of myosin-binding site of actin filaments. The assignment of the domains A and B was more difficult, and there was an argument:[40),42] The issue was whether assign actin to the domain B or not. To clarify the situation, the better images of the actin-tropomyosin complex were collected using a minimum dose method.[43] To objectively assign actin, the cross-correlation between the actin filament and its complex with myosin S1 was calculated as a function of rotation angles, shift distances and polarity of filament.[44] The cross-correlation function gave a unique maximum and the interface between actin and myosin could be determined unambiguously as shown in Figs. 5A–C.

Figure 4C shows the visual validation of the assignment of actin. The top panels show the actin-tropomyosin-myosin S1 complex on the left, and the actin-tropomyosin complex without myosin S1 on the right. After aligning two structures according to the results of the cross-correlation analysis, the weighted averages of densities of two structures were calculated, and are shown in the bottom three panels.

These models were calculated as follows:

$$\{\text{Actin-tropomyosin-myosin S1}\} \times (1\text{-w}) + \{\text{Actin-tropomyosin}\} \times \text{w}, \quad [1]$$

where w is a weighting factor.

Following the panels in a counterclockwise manner, the weighting factor increases. Thus, the volume corresponding to the myosin S1 will decrease, on the other hand that corresponding to actin should be constant, because actin is contained in both structures. The objective alignment of two structures in this manner allowed the unambiguous assignment of actin and myosin S1. It showed that both of the domains A and B correspond to actin-tropomyosin. This new assignment was supported by the structure relationships of actin, myosin, and tropomyosin revealed by electron cryo-microscopy (cryo-EM).[45] The structure as assigned as actin was similar to that of F-actin structure revealed by cryo-EM at higher resolution enabling the assignment of α-helices[46)–48] and that of the actin-tropomyosin part in the actin-tropomyosin-myosin complex revealed by cryo-EM at 8 Å resolution.[49] Also, the shapes of actin and myosin S1 thus determined are consistent with X-ray crystallographic structures of actin monomer,[50] and myosin S1,[51),52] respectively. Also, the interface between actin and myosin is consistent with that determined by docking the crystal structure of myosin S1 into the actin-tropomyosin-myosin S1 complex.[45),52]

Figures 5A–C show the mode of the interaction between actin filament and myosin. Myosin mainly interacts with the actin protomer (monomer) on one strand. The myosin-binding sites correspond to the domains A2 and B2 shown in Fig. 4B. Figure 5D shows the corresponding actin-binding site on myosin surface. Thus, the myosin-binding sites on actin was established for the first time: One myosin head mainly bound to one actin protomer (monomer) on one strand of the actin double helix. Also, deducing from the arrowhead appearance and the triangular shape of actin, the polarity of actin-containing filaments in sarcomere was determined: The convex surface of actin as seen in Fig. 2D was shown to point towards the Z-band.

The remaining task to obtain the evidence for the steric blocking mechanism was to show the precise location(s) of tropomyosin on actin. Sixteen years later, this was eventually achieved by applying single-particle analysis to cryo-electron micrographs of actin-tropomyosin-troponin: On some of actin protomers (monomers), the myosin-binding sites were shown to be covered by tropomyosin in the absence of Ca^{2+}. However, it was totally unexpected that only the carboxyl-terminal one-third of tropomyosin molecule shifted as described below in the section 4.4.

3. ATP-binding site (ATPase site) of myosin

3.1. Development of avidin-biotin system for electron microscopy. We developed a new labeling method for electron microscopy to visualize the specific site of myosin using the avidin-biotin system.[53] The size of avidin with the molecular mass of 70 kDa is ~5 nm in diameter, which is large enough

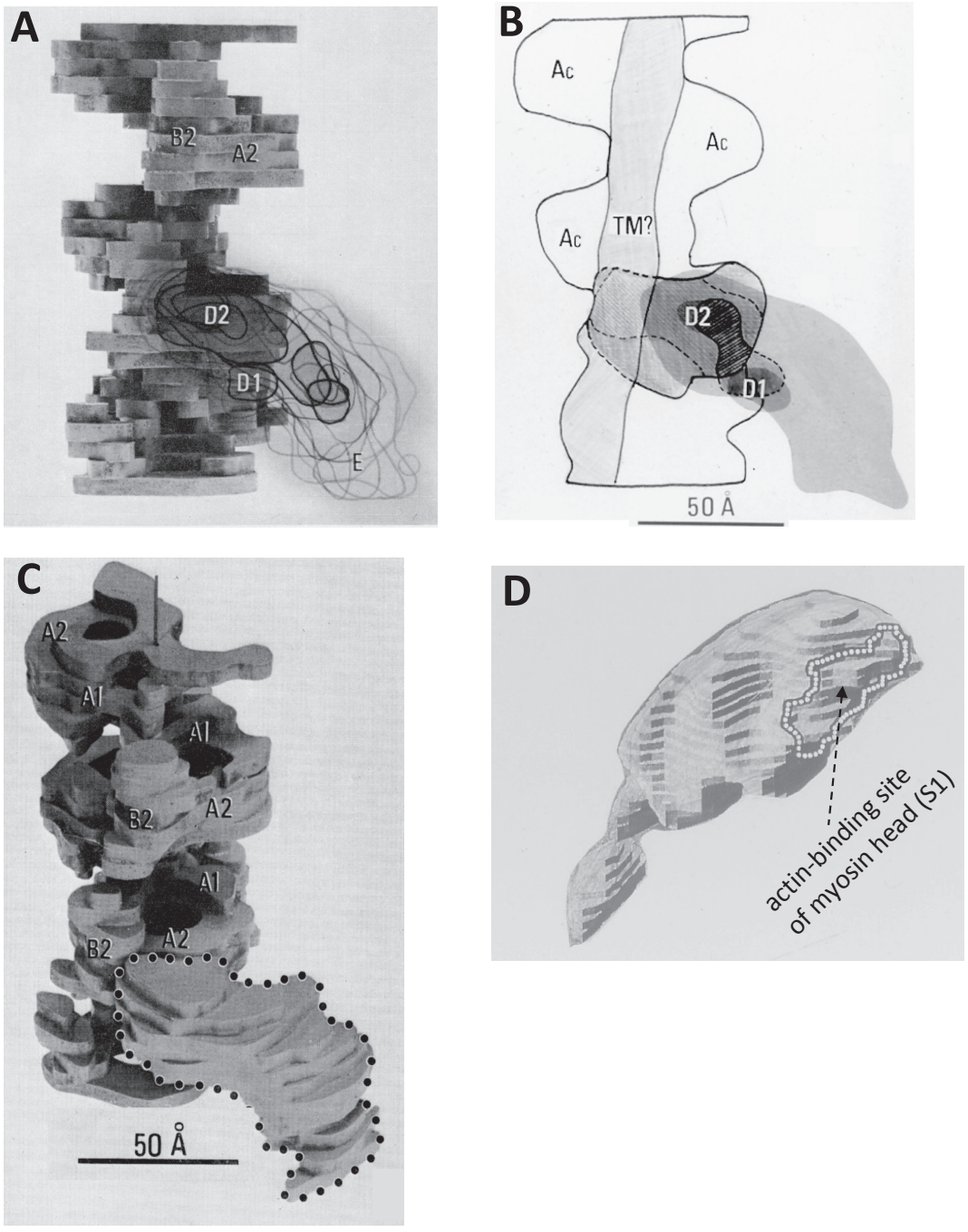

Fig. 5. The interaction of actin filament with myosin head, and actin-binding site of myosin.[44] A–C. Myosin head interacts with the actin protomer (monomer) on one strand. The myosin-binding sites correspond to the domain A2 and B2. D. The corresponding actin-binding site on the surface of myosin head. The top of illustrations corresponds to the M-line side.

to be visualized directly by electron microscopy. Because biotin is a small molecule (molecular mass: ~244 Da), the protein structure is most likely to be unaffected by the biotinylation. Taking advantage of high affinity of avidin to biotin ($K_d \sim 10^{-15}$ M), the biotinylated site of the target protein can be visualized by attaching avidin.

To visualize the location of one of the reactive thiols in the myosin head (Cys-707, so called SH1), biotinylated iodoacetatic acid, N-iodoacetyl-N-bioti-

nylhexylenediamine, was synthesized and attached to the myosin head. The complex of biotinylated myosin and avidin was readily formed, and the attachment site of avidin on the myosin head was 13 nm away from the head-rod junction, indicating the location of the SH1. This reagent and biotinylated maleimide turned out to be popular due to their general applicability, and now are commercially available.

To visualize ATP-binding site of myosin, biotinylated photoreactive analog of ATP, was synthesized.[54),55)] The structure of ADP analog was:

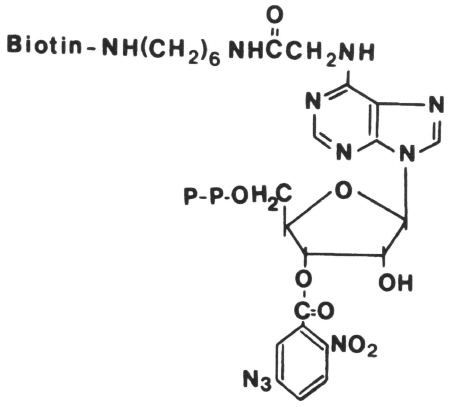

The ATP analog was hydrolyzed to the ADP analog by incubation with myosin S1. The ADP analog was then trapped into the ATPase site of myosin S1 in the presence of vanadate (Vi) to form the stable S1-ADP-Vi complex, and covalently photo-crosslinked to the site by ultraviolet illumination. After adding avidin to the modified S1-ADP-Vi, the complex of actin-tropomyosin and S1-ADP-Vi, of which the biotinylated ADP was associated tightly with avidin, was observed by electron microscopy.

3.2. Location of ATP-binding site of myosin. Figures 6A and 6B show the end-on views of the transparent model and that without avidin decoration, respectively. In the reconstructed image, there was a protrusion on the outer surface of myosin S1. Figure 6C shows the schematic illustration of Fig. 6A.

It was noticed that the association of myosin S1-ADP-Vi to actin-tropomyosin was not so tight as that of myosin S1 without adenine nucleotide shown in Figs. 4B and 6B: There were clear grooves between actin and myosin S1 as indicated by the arrows in Fig. 6A. This is consistent with the weaker affinity of S1-ADP-Vi to actin filaments. The discontinuous column-like structures, interpreted as a candidate for tropomyosin, were observed near the grooves of actin double helix as shown in Fig. 6D. According to a three-state model of Ca^{2+}-regulation, this position of tropomyosin represents that of an "open" state or an R state as shown in the right panel of Fig. 15.

Figure 6E shows the spatial relationship between important sites of myosin S1: The ATP-binding site is ~4 nm away from actin-binding site, these sites locate on the opposite side of the surface of myosin S1. This position is favorable for ATP binding, being located on the outside of the actin-myosin complex. When ATP binds to the actin-myosin complex, the affinity of actin to myosin-ATP decreases and the complex dissociates into actin and myosin-ATP. Because the distance between the ATP-binding site and the actin-binding site is 4 nm, the effect of ATP binding is transferred allosterically to the actin-binding site. Later, the crystal structure of myosin S1 was solved,[51)] and it supported the positions of ATP and the reactive cysteinyl residue (SH1) revealed by avidin-biotin method.[53)–55)] The relationships of the actin-binding site, the ATP-binding site, and SH1 of the myosin head was also supported by the structure of the actin-tropomyosin-myosin S1 complex, into which the atomic structure of myosin S1 was docked.[52)]

Although the tilting of the whole myosin head was proposed as a working hypothesis for the mechanism of muscle contraction,[56)] such a tilting or tilt conformation of the whole myosin head was not observed experimentally in the vertebrate muscles[41),57)–62)] except for the pioneering three-dimensional image reconstruction of actin-myosin complex.[17)] However, Figs. 4A, 5A–C, and 6D show that the myosin head or S1 can be divided into three parts, the main region, the neck region, and the bending region that is connected to the tail of myosin. Because the neck region and the bending region look tilted and do tilt as described below, the non-tilted conformation of the main region does not necessarily conflict with an original working hypothesis of the tilting of myosin head.[56)] Moreover, the bent or curved form of myosin head was also observed by electron microscopy of thin sections of a small crystal of myosin S1.[63)]

In the rigor complex, the axis of the main region is not tilted and almost perpendicular to the axis of actin helix.[55),57)] From this observation, we suggested that muscle contracts by tilting the bending region of myosin S1 rather than the main region.[55)]

3.3. ATP-induced conformational changes of myosin head. In the right panel of Fig. 6E, two myosin heads are depicted differently. One is more bent than the other.

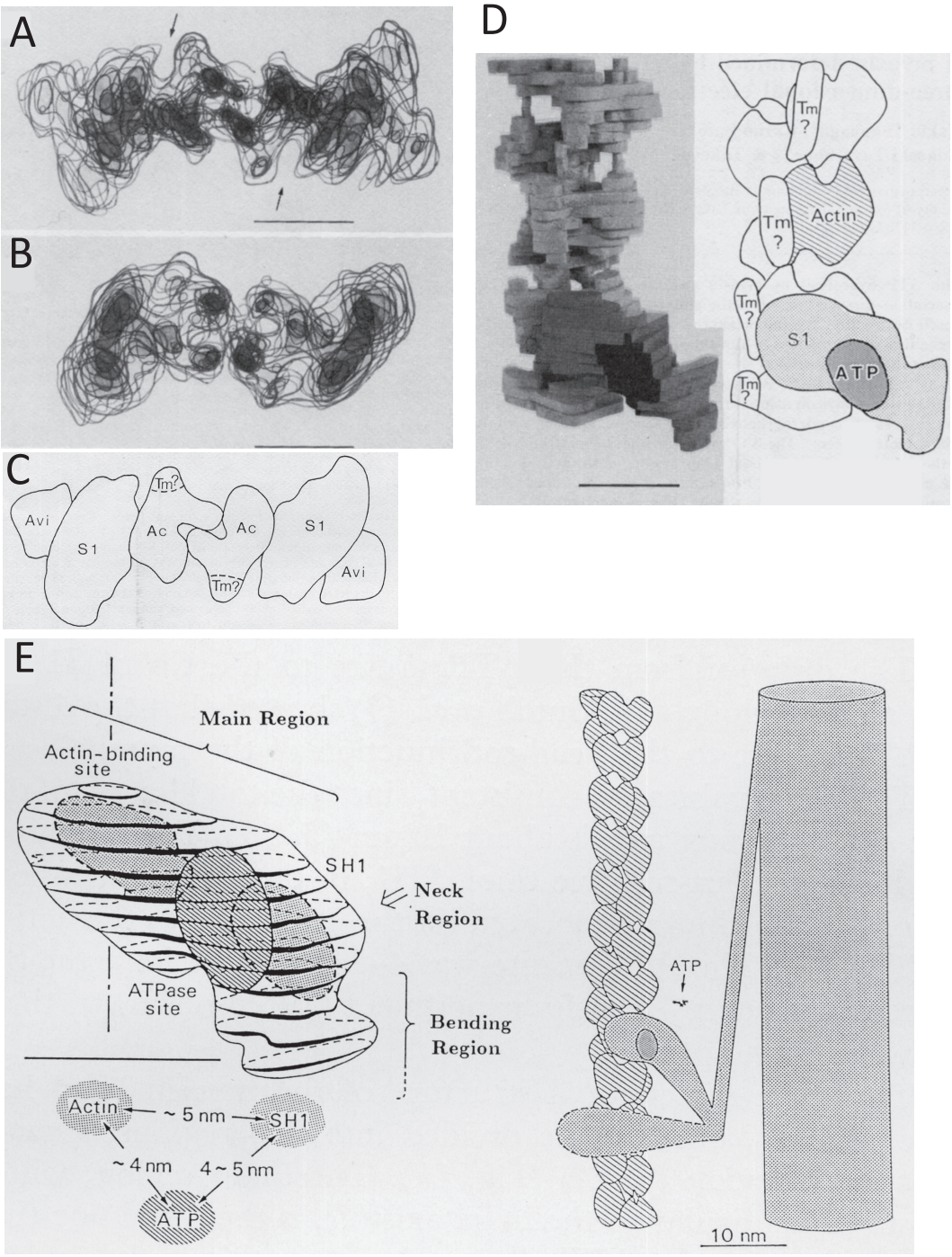

Fig. 6. Location of ATPase site of myosin and its relation to the actin-binding site as revealed by electron microscopy of negatively stained specimens by assuming the helical symmetry of specimens.[55] A. The end-on view of the transparent model of actin-tropomyosin-myosin S1-ADP-Vi and avidin. A protrusion on the outer surface of myosin S1 corresponds to avidin. B. The end-on view of actin-tropomyosin-myosin S1 without avidin. C. The schematic illustration of A. D. The discontinuous column-like structures, interpreted as a candidate for tropomyosin in an R-state or an "open" state (right panel of Fig. 15) observed near the grooves of actin double helix. E. The spatial relationship between the actin-binding site, the ATPase site, and reactive thiol (SH1, Cys-707) determined by the developed avidin-biotin system is shown in the left panel.[53)–55)] In the right panel, two myosin heads are depicted differently. One is more bent than the other. The ATP-induced changes of the angle of the bending region against the main region were shown experimentally.[64)–71)]

Three lines of evidence revealed the ATP-induced changes of the angle of the bending region or the lever arm against the main region. Firstly, when myosin heads were examined by electron microscopy using a shadow-casting technique, ~30% of the total heads are bent in the absence of ATP. With ADP and vanadate (Vi), myosin forms the stable myosin-ADP-Vi complex, in which ~50% of heads were bent.[64] Secondly, small-angle synchrotron X-ray scattering of papain-treated chicken S1, which fully retains light chains, showed that the head becomes more compact by the addition of ADP and vanadate. Modeling based on X-ray scattering data indicated that the bending angle increased from 40 degree to 65–70 degree by the addition of ADP and vanadate.[65] Thirdly, the fluorescence resonance energy transfer (FRET) from the BFP connected to carboxyl-terminus of myosin S1 to the GFP connected to the amino-terminus of myosin S1 decreased rapidly, but it recovered slowly due to ATP hydrolysis, indicating the swing of the lever arm.[66] While the nucleotide-free myosin head shows the high FRET efficiency, the head with ADP and vanadate showed the low FRET efficiency, which is similar to that with ATP. The calculated distance between BFP and GFP increased from 3.6 nm to 5.3 nm, when ADP and vanadate were added to the nucleotide free myosin head. This shows that the myosin-ADP-Vi assumes a state similar to the myosin-ADP-phosphate (M**-ADP-Pi). This is consistent with biochemical data.[67] X-ray crystallography also showed the tail part of the myosin head in the myosin-ADP-Vi complex is more bent[68] than that of myosin-ADP[69] and nucleotide free myosin.[51]

The conformation of the myosin-ADP-phosphate complex is important, because it represents the pre-stroke form. The phosphate release from this complex triggers the working stroke. By combining the crystal structures of GFP and myosin head with the results of FRET measurements, the swing of the lever arm was demonstrated.[66),70] X-ray diffraction and mechanical measurements of muscle fibers also indicate active tilting of myosin heads.[71]

4. Three-dimensional structure of actin-tropomyosin-troponin

4.1. Visualization of troponin on actin filaments (F-actin). Troponin plays a central role in the calcium-regulation of muscle contraction: Troponin is the sole calcium-binding component of thin filaments (actin-tropomyosin-troponin complex) of striated muscles.

Thin filaments without troponin support contraction irrespective of calcium concentration. Therefore, the one of the most important functions of troponin is the inhibition of contraction at low Ca^{2+} concentrations. The calcium ions released from endoplasmic reticulum[72] bind to the calcium-binding subunit of troponin (troponin-C (TnC), ~18 kDa), and the inhibition by troponin is neutralized to trigger muscle contraction.

The three-dimensional positions of troponin on actin-containing filaments had not been worked out in spite of its great importance. This is because a molar ratio of actin and troponin is 7:1.[7] Therefore, the axial repeat of the troponin molecules (~38 nm, 5.5 nm × 7) along the actin filament does not coincide with the crossover repeat of the actin filament (~36 nm, 5.5 nm × 6.5). This mismatch of periodicity prevents the exploitation of the helical symmetry to reconstruct three-dimensional images of the total structure including troponin.

Until 2001, the movement of tropomyosin was determined by assuming the helical symmetry of actin-containing filaments.[34),73–77] Squire and Morris[78] raised the important question: The actin filaments contain troponin, but the helical symmetry of actin imposed in three-dimensional reconstructions did not account for the different troponin axial repeat of ~38 nm, and in the reconstructions, the troponin with a larger mass than tropomyosin was effectively "added" over a structure with actin helical symmetry and would affect the position of tropomyosin.

To address this issue, two approaches were adopted. One way was to remove TnT from the actin-tropomyosin-troponin complex.[79] It is TnT that determines a ratio of 7:1 for actin and troponin. Without TnT, the ratio of actin and Tn-(I+C), which is a binary complex of TnI and TnC, becomes 1:1 instead of 7:1. Thus, Tn-(I+C) binds to each of actin protomers (monomers). The filaments consist of actin, tropomyosin, and Tn-(I+C) in a ratio of 7:1:7 can be three-dimensionally reconstructed using helical symmetry of actin. In this case, the only assumption made was the quasi-equivalence of 7 repeating motifs of tropomyosin.

The second approach was more physiological: Single particle analysis[80)–82] was applied to the electron cryo-micrographs of the full complex of actin-tropomyosin-troponin. This method allows three-dimensional reconstruction without imposing the helical symmetry. In electron cryo-microscopy (cryo-EM),[83] the hydrated specimens themselves can be observed without staining, and Ca^{2+} concen-

tration can be controlled by EGTA. In single particle analysis, filaments were divided into short segments, which were then treated as "single particles". After the orientation of "single particles" is determined, two-dimensional images are combined to reconstruct the three-dimensional image in a similar manner to the CT-scan method.

The structures in the presence and absence of calcium could be determined at about 30-Å resolution. The use of highly coherent electron beam generated by a cold field-emission gun (cFEG) helped minimize the blurring due to defocusing used to enhance contrast of the images.[84]

Figure 7A shows the reconstructed images of actin-tropomyosin-troponin. In Fig. 7B, the density due to actin was subtracted to show up troponin and tropomyosin. Troponin was visualized for the first time on actin filaments.[84] Two troponin molecules on the two long-pitch actin helices were shown to be staggered by ~27.3 Å along the actin filament, and indicated by hard brackets in Figs. 7A–B. This was the first direct evidence for the 27.3-Å staggering of troponin, and supported the model (Fig. 1C) proposed by Ohtsuki.[25] In invertebrate muscles, it has been known that their X-ray diffraction patterns were only consistent with the troponin staggering of ~27.3 Å.[85)–88)]

4.2. Ca^{2+}-induced shift of troponin. The main body of troponin (troponin head) shifted towards the outer domain of actin and covered the myosin-binding sites of actin at low Ca^{2+} concentrations as shown in Fig. 7B. A curly bracket in Figs. 7A–B indicate the typical image of actin at high Ca^{2+} concentrations. In Fig. 7E, the myosin-binding sites[89] of actin are shown in various colors (residues 1–4, red; 93–96, orange; 24–28, yellow; 340–346, green; 144–148, cyan; 324–336, blue) in solid models. Except for residues 324–336, which belong to the inner domain of actin, these residues belong to the outer domain. The shift of troponin head is also supported by the FRET measurements.[90]

To assess the contribution of the troponin head to X-ray diffraction diagrams, the computed diffraction patterns of our three-dimensional images were examined. When the computation was done after the removal of the troponin head from the total structure, the meridional reflections with spacings of 1/380, 1/190, 1/127, and 1/95 $Å^{-1}$ almost disappeared, confirming that these reflections mainly originated from the troponin head. These reflections were also observed in the X-ray diffraction pattern of invertebrate muscles.[87] The intensities in off-meridional regions between the second (1/190 $Å^{-1}$) and fifth (1/69 $Å^{-1}$) actin layer-lines also became weaker. The troponin head, therefore, contributed also to the off-meridional actin layer-lines. Thus, the earliest change in the second layer-line of X-ray diffraction[91] was shown to partially reflect the shift of the troponin head. It is natural that the earliest structural changes during the activation of muscle reflected the movement of the troponin head, which binds Ca^{2+}.[19]

4.3. Emergence of the troponin arm. The shape of the troponin head also changed according to Ca^{2+} concentration. An eminent protrusion emerged from the main body of the troponin head at low Ca^{2+} concentrations, as shown in the left panels of Figs. 7D–E. Its molecular mass estimated from its volume was ~6 kDa. The protrusion, named troponin arm, associated intimately with the actin filament. It covered the region where three actin protomers (monomers) meet. This region was not covered by troponin or tropomyosin at high Ca^{2+} concentrations, and indicated by an asterisk in the right panel of Fig. 7E. The corresponding position at low Ca^{2+} concentrations was covered by the troponin arm, and indicated by a cross in the left panel. The position of the troponin arm was similar to that of Tn-(I+C) in the complex of actin, tropomyosin, and Tn-(I+C) at low Ca^{2+} concentrations.[79]

The troponin arm had no obvious counterpart in crystal structures of the troponin head.[92] Because the atomic structures of the troponin head showed almost all regions except for the COOH-terminal region of troponin-I (TnI), it was thought that this region may correspond to the troponin arm, which may be mobile and more difficult to be visualized in X-ray crystallographic structures. Therefore, NMR spectroscopy was applied to the troponin head (~52 kDa) to solve the atomic structure of the troponin arm. Figure 7C shows the solution structure of the troponin arm, of which the details will be described in the section 5.

4.4. Differential shift of tropomyosin. Most unexpectedly, tropomyosin did not smoothly follow the long-pitch actin helices at low Ca^{2+} concentrations, whereas it did at high Ca^{2+} concentrations. This indicates that the assumption of the pseudo-equivalence of 7 repeating motifs of tropomyosin on actin filaments can be justified only at high Ca^{2+} concentrations.

In Fig. 8A, a structural unit containing seven actin monomers, one tropomyosin, and one troponin is divided into 7 blocks. The average position of the

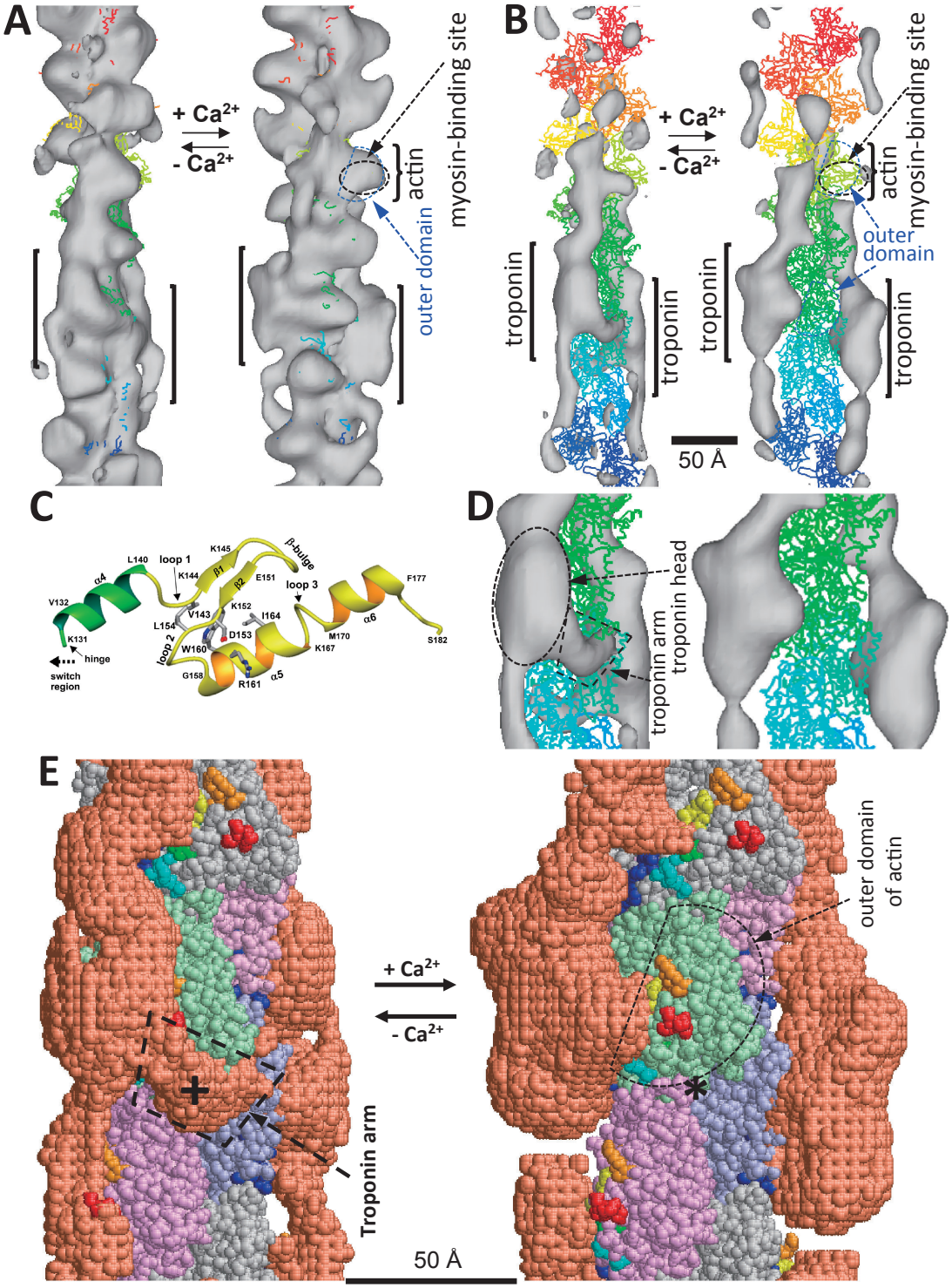

Fig. 7. Three-dimensional models of actin-tropomyosin-troponin[84] as revealed by electron cryo-microscopy *without* assuming helical symmetry, and the atomic structure of the troponin arm.[102] A. The structures of actin-tropomyosin-troponin. The outer domain and the myosin-binding sites of actin are indicated by arrows. B. The structures after subtracting the density due to actin, of which the atomic structure[50] in wire format. C. The atomic model of the troponin arm.[102] D. Enlarged view of the panel B. E. The models of actin-tropomyosin-troponin. A cross indicates the center of troponin arm, and an asterisk indicates the corresponding position, where three protomers meet. The myosin-binding sites[89] on actin are shown in various colors (red, orange, yellow, green, cyan, and blue).

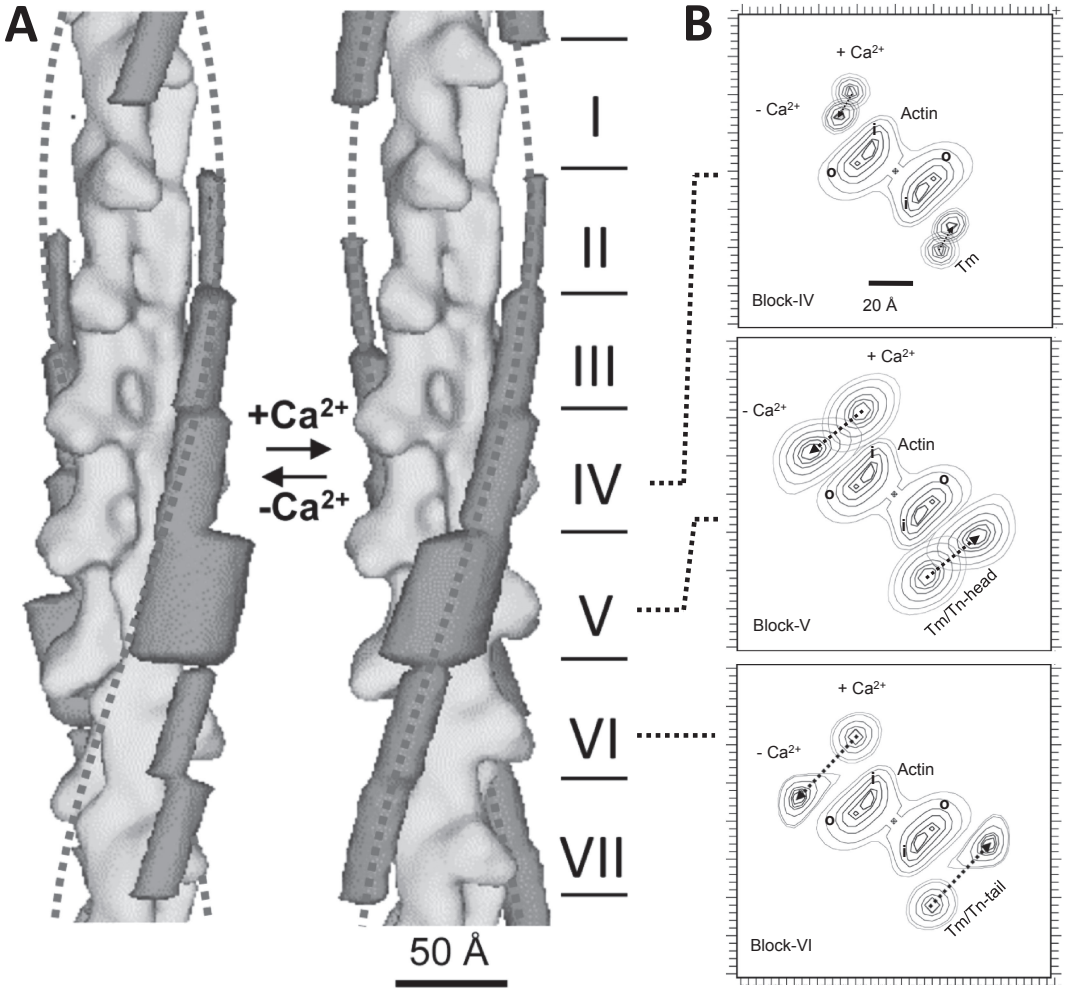

Fig. 8. The differential shift of tropomyosin at low Ca^{2+} as revealed by single particle analysis of electron cryo-micrographs.[84] A. Three-dimensional models of actin-tropomyosin-troponin at low Ca^{2+} (left panel) and at high Ca^{2+} (right panel). The whole structures were divided into seven blocks so that each of them contains one actin monomer, and the densities due to tropomyosin-troponin were averaged and shown in dark gray. The block I and VII correspond to the NH-terminal and COOH-terminal regions of tropomyosin, respectively. The dotted lines show smooth helices to indicate the typical position of tropomyosin at high Ca^{2+}. The extent of Ca^{2+}-induced shifts differed between blocks. The M-line locates upwards. B. The top views of the panel A from the M-line side. By the depletion of Ca^{2+}, tropomyosin-troponin moved anticlockwise. The extent of movement differed: about ~35 Å in the block V and VI, but was small in the block II, III, and IV. After the shift of tropomyosin-troponin, the outer domain of actin and the myosin-binding sites were covered: The evidence for the steric blocking model was provided.

tropomyosin and troponin in each block is shown in dark gray, while the density due to actin is shown in light gray. Only the COOH-terminal one-third of tropomyosin, which is in blocks V, VI, and VII (numbered from the pointed end or minus end), shifted by ~35 Å. However, the NH-terminal one-half of tropomyosin did not move much (~10 Å). The small extent of the shift in NH-terminal region was consistent with the results of FRET measurement: The fluorescent dyes labeled to various parts of this region did not move significantly.[93),94)] There is, however, some inconsistency between the large shift of the COOH-terminal region of tropomyosin and the results of FRET measurements that showed no significant movement of the dyes labeled to the corresponding region of tropomyosin.[95)] More work is required to scrutinize the origin of inconsistency.

Figure 8B shows the top views of the Fig. 8A, that is, the end-on views from the M-line side. By the depletion of Ca^{2+}, tropomyosin and/or troponin moved anticlockwise. However, the extent of movement differed as stated above: It was ~35 Å in the

block V, or VI, but was as small as ∼10 Å in the block II, III, IV. The direction of the shift was favorable to cover the outer domain of actin, where the myosin-binding sites locate. Thus, the evidence for the steric blocking model was eventually obtained. However, the extent of blocking depended on the region of tropomyosin, and the situation was not so simple as the original model proposed.

The biochemical data also showed the inhibition of actin-activated ATPase by tropomyosin and troponin at low Ca^{2+} concentrations is not perfect and ∼30% of activity remains.[96] The extent of the inhibition depends also on ionic strength of solution and the concentration of ADP and phosphate.[97]

5. Atomic structure of the troponin arm (mobile domain)

5.1. NMR spectroscopy of troponin and the atomic structure of the mobile domain. Troponin and tropomyosin on actin filaments constitute a Ca^{2+}-sensitive switch that regulates the contraction of striated muscles through a series of conformational changes within the actin-based thin filament.

Troponin consists of three components: An inhibitory subunit (troponin-I, TnI), a Ca^{2+}-binding subunit (troponin-C, TnC), and a tropomyosin-binding subunit (troponin-T, TnT). Ca^{2+}-binding to TnC is believed to weaken interactions between troponin and actin, and triggers a conformational change of the troponin. The COOH-terminal region of TnI (residues 130–182) is indispensable for full inhibitory activity[98)–100] and contributes 65% of the total inhibitory activity.[98),101] However, the atomic structure of this region was not obvious in the crystal structure of the troponin head.[92]

NMR spectroscopy was applied to solve the atomic structure of the troponin head.[102] Tn-(T_2+I+C), the ternary complex of TnT_2, TnI, and TnC, was reconstituted. The tail part of troponin, TnT_1,[103] was removed to facilitate tumbling motion of the complex in solution for the acquisition of better NMR spectra. Among three components, chicken skeletal TnI was uniformly labeled with ^{15}N and/or ^{13}C using the *E. coli* expression system. Even though the molecular mass of Tn-(T_2+I+C) is ∼52 kDa and is too large for the conventional NMR spectroscopy, good spectra of the residues 131–182 of TnI could be obtained at low and high Ca^{2+} concentrations. This suggests that the residues 131–182 of TnI are much more mobile than the other parts of Tn-(T_2+I+C). The Ca^{2+}-induced changes in the line shape of NMR spectra suggested that the tumbling movement of the mobile domain in Ca^{2+}-loaded complex was more restricted: The residues 131–182 associated with the main body of troponin as indicated by the chemical shift.

The residues 131–182 represent the most mobile segment of the troponin head, and this segment was called "the mobile domain", because it is mobile, but forms a compact globular domain.

The shape of the mobile domain looked similar to that of the troponin arm shown in Figs. 7D–E. The molecular mass of ∼6.1 kDa is nearly the same as the value estimated from the volume of the troponin arm (∼6 kDa). The mobile domain was identified with the troponin arm by comparing the outline of the atomic structure of the mobile domain with the density map of the troponin arm in the actin-tropomyosin-troponin at low Ca^{2+} concentrations (left panels of Figs. 7B and D, and Fig. 9C). Also the estimated molecular mass of the troponin arm was almost equal to that of the mobile domain.

Figure 9A and Fig. 7C (in color) show the ribbon-and-stick model of the atomic structure of the mobile domain in the Tn-(T_2+TnI+TnC) ternary complex. The size (40 Å × 20 Å × 15 Å) and the outline of the mobile domain were similar to those of the troponin arm revealed with cryo-EM of the actin-tropomyosin-troponin at low Ca^{2+} concentrations.[84] The whole mobile domain can tumble independently in the ternary complex, with a pivot (hinge) located between Gly127 and Lys131 (human cardiac Gly160 and Lys164).

The residues 143–167 formed a mini-globular domain, of which the general architecture resembled a zinc finger DNA-binding motif found in several transcription factors.[104] Usually a short peptide tends to be unfolded, but the mobile domain and a zinc finger are exceptional examples. The stability of the mobile domain was found to be marginal: Chemical shift difference analysis, in which the difference between the chemical shift of the mobile domain and that of random coil is examined, was exploited to establish the secondary structure of the mobile domain.[102] This suggests that the some population of the mobile domain of the Tn-(T_2+TnI+TnC) ternary complex may be unfolded and that it would be prudent to concentrate the complex by ultrafiltration refraining from lyophilization. Also, the monodispersity of the reconstituted ternary complex was confirmed with native gel electrophoresis and gel-filtration.

The side chains of several residues (Val143, Leu154, Trp160, Asp153, Ile164, and Arg161)

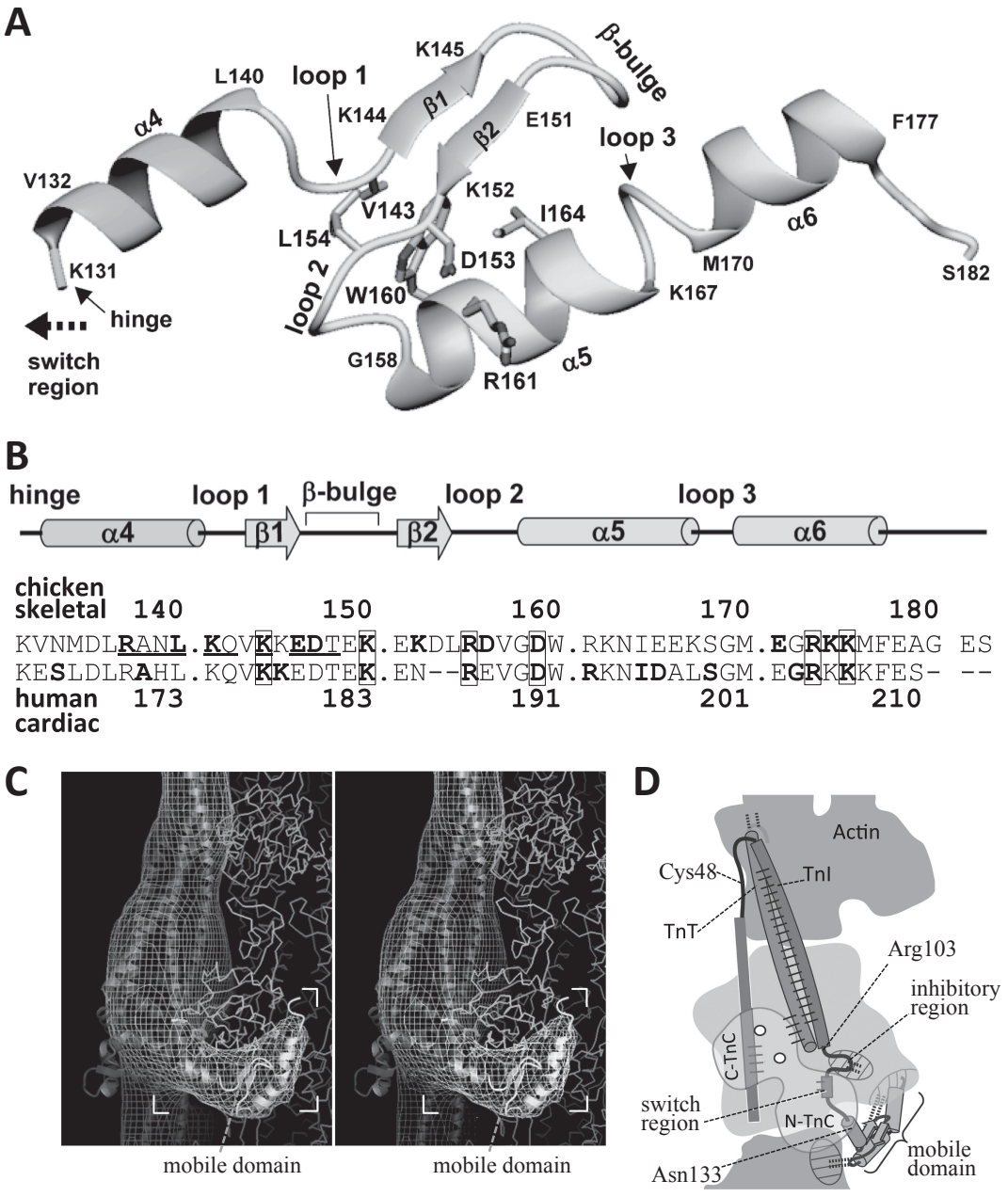

Fig. 9. The atomic structure of the mobile domain of troponin as revealed by NMR spectroscopy of the ternary complex of TnT_2, TnI and TnC.[102] A. The atomic structure of the mobile domain (residues 131–182 of TnI) in the ternary complex. Figure 7C shows the same structure in color. B. Summary of secondary-structure elements, the sequence of the mobile domain, and that of the corresponding region of the human cardiac muscle. The residues that showed Ca^{2+}-induced changes in chemical shifts are underlined. The residues that interact with actin are shown in bold letters. The numbering shown in the upper line is for skeletal troponin-I. The numbering in the lower line is for the human cardiac one. The residues related to human cardiomyopathy[106] are shown in bold letters, and are enclosed with boxes, if they were also involved in the interaction with actin. C. A stereo pair to show the mobile domain (in ribbon format) docked into the image of the troponin arm (net of contour lines). Atomic structure[50] of actin is shown in wire format. The residues found to interact with actin were shown in bold letters in the upper line of the panel B. The interaction was mainly electrostatic. D. Summary of the general relation of actin with troponin at low Ca^{2+} concentrations. The mobile domain of TnI, together with the inhibitory region of TnI, holds the COOH-terminal region of actin. The dotted lines indicate the interactions between TnI and actin. The solid lines indicate the interactions within troponin.

stabilizing a mini-globular hydrophobic core are shown in stick model in Figs. 7C and 9A.

Figure 9B shows a summary of secondary-structure elements, the sequence of the mobile domain, and that of the corresponding region of the human cardiac muscle. The residues that showed Ca^{2+}-induced changes in chemical shifts of NMR spectra are underlined: These residues are the candidates for the Ca^{2+}-enhanced interaction with the main body of the troponin head. The numbering shown in the upper line is for skeletal troponin, of which the TnI is smaller than that for cardiac one by ~30 residues due to the insertion at the NH-terminal region of the cardiac one.

5.2. Fitting of the mobile domain to the troponin arm of actin-tropomyosin-troponin. Figure 9C shows a stereo pair to visualize how well the atomic structure of the mobile domain (in ribbon format) can be docked into the electron cryo-microscopic image of the troponin arm (net of contour lines). Atomic structure of actin[50] is shown in wire format. Three-dimensional cryo-EM images of actin filaments decorated with the recombinant mobile domain, of which the COOH-terminus was fused with GFP showed that the COOH-terminus of the mobile domain corresponds to the tip of the troponin arm.[102] This information helped unambiguous determination of the orientation of the atomic model of the mobile domain for docking. The general shapes of the troponin arm and the mobile domain were similar, if not identical. It is conceivable that the structure of the mobile domain becomes more stable through its interaction with actin.

Fifteen residues shown in bold letters were found to interact with actin (the upper line in Fig. 9B). The interaction between the mobile domain and actin was mainly electrostatic: The residues are charged except for leucine-140, and their actin counterpart was oppositely charged.

Figure 9D summarizes the general relation of actin with troponin at low Ca^{2+} concentrations. It emphasizes the importance of the interactions of actin with the mobile domain and inhibitory region of TnI at low Ca^{2+} concentrations: The mobile domain, together with the inhibitory region, holds the COOH-terminal region of actin.

Figure 10 schematically shows the Ca^{2+}-induced changes in the mode of interaction between actin and troponin.[105] When Ca^{2+} binds to the N-domain of TnC (step (1)), the hydrophobic pocket opened, and the association between the switch region (second TnC binding site of TnI) and the N-domain of TnC becomes tighter (step (2)). Then, the inhibitory region and the mobile domain of TnI detach from actin (step (3)). This detachment is the key step for the triggering of the activation of muscle contraction. Thus, the regulatory machinery consists of five members, which are the N-domain of TnC, the inhibitory region, the switch region, and the mobile domain, and actin. Actin is, therefore, not just a target of Ca^{2+}-regulation but is an important component of the Ca^{2+}-switch. The mobile domain shuttles between actin (at low Ca^{2+} concentrations) and the main body of troponin (at high Ca^{2+} concentrations).

5.3. Medical implications of the interaction of the mobile domain with actin. The mobile domain (troponin arm) is a hot spot of mutations, which cause human familial cardiomyopathy. Eight mutated residues located at the interface between the mobile domain of TnI and actin. The patterns of surface electrostatic potential were complimentary. In the human cardiac sequence (lower line in Fig. 9B), the residues related to human cardiomyopathy[106] are shown in bold letters, and are enclosed with boxes if they were also shown to be involved in the interaction with actin.

Most of the cardiomyopathy mutations occur in the charged residues of the mobile domain, which suggests the functional importance of the electrostatic interaction. Indeed, the recombinant mobile domain fused with GFP binds more strongly to actin filaments at lower salt concentrations.[102]

6. Head-to-tail interaction of tropomyosin

6.1. Crystal structures of tropomyosin junction. Actin filaments are usually associated with tropomyosin. However, at the leading edge of the cells actin filaments tend to be tropomyosin-free, and less than one fourth of actin filaments have tropomyosin bound.[107] Tropomyosin protects actin filaments from spontaneous fragmentation,[108] and stabilizes actin filaments by inhibiting the dissociation of actin protomers (monomers) from the end of filaments[109] or by competing with ADF/cofilin, which destabilizes actin filaments.[110]

Tropomyosin is a long protein (~40 nm) with two α-helical polypeptide chains that form a coiled coil in a parallel orientation by winding around each other in a left-handed superhelix. Tropomyosin molecules lie along the actin helix and successive molecules interact in a head-to-tail manner, and the junction is formed between the COOH-terminus of one tropomyosin and the NH-terminus of the next.

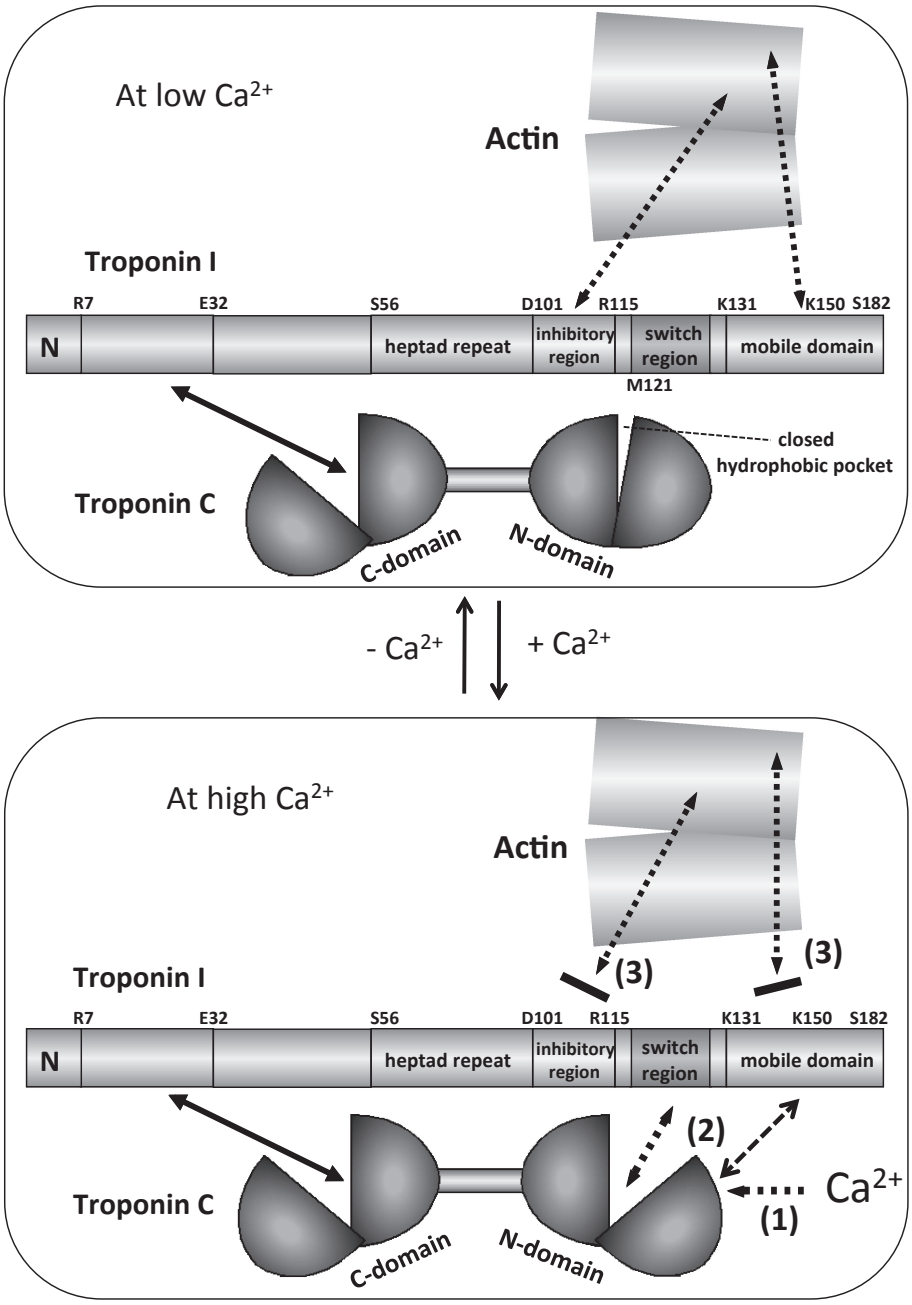

Fig. 10. Schematic model of the Ca^{2+}-induced changes in the mode of interaction between actin and troponin.[105] Step 1: Ca^{2+} binds to the N-domain of TnC, and the hydrophobic pocket opened. Step 2: the association between the switch region of TnI and the N-domain of TnC becomes tighter. Step 3: the inhibitory region and the mobile domain of TnI detach from actin, and this detachment is a key step to trigger the activation of muscle contraction. Note that actin is not just a target of Ca^{2+}-regulation, but is an important component of the Ca^{2+}-switch. The mobile domain of TnI shuttles between actin (at low Ca^{2+} concentrations) and the main body of troponin (at high Ca^{2+} concentrations). Solid arrows indicate permanent interactions, whereas the dotted arrows indicate regulated interactions.

The capability to form the head-to-tail junction is crucial for function, because only tropomyosins that form the junction can bind to actin filaments.

The sequence of tropomyosin contains seven-residue repeats called "heptad" (designated *a*-*b*-*c*-*d*-*e*-*f*-*g*),[111),112)] of which the examples are shown in lower half of Fig. 11A. To form a stable left-handed coiled

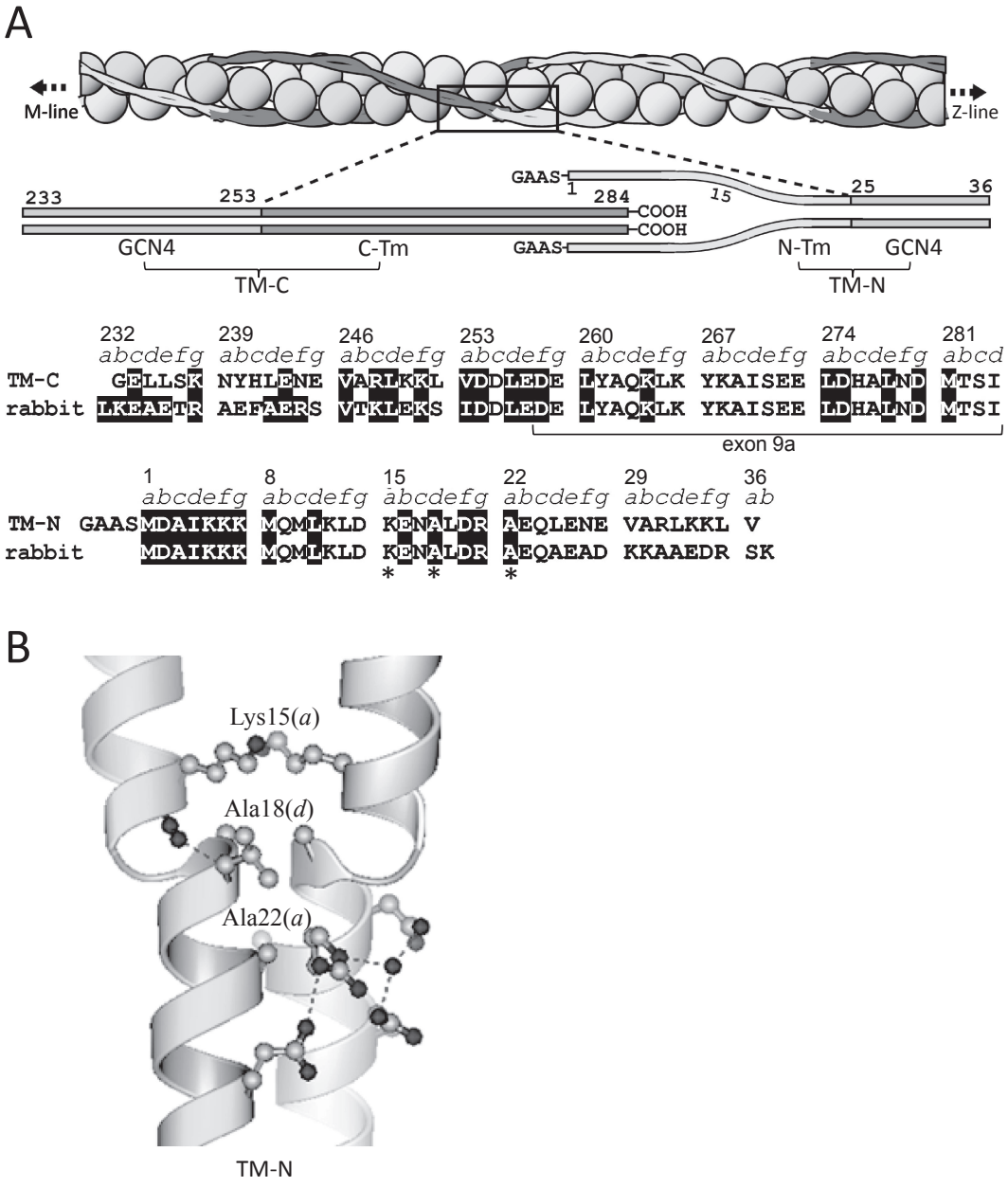

Fig. 11. A schematic model of actin-tropomyosin, tropomyosin fragments, and atomic structure of NH-terminal region of tropomyosin.[119] A. Together with models, the amino acid sequence of tropomyosin fragments TM-C and TM-N (upper lines) and the corresponding sequences of rabbit skeletal α-tropomyosin (lower lines) are shown. Asterisks indicate the key residues responsible for the splaying of the coiled coil. B. In the binary complex of TM-N and TM-C, the α-helices of TM-N were splayed apart from Met-1 to Lys-15. Ala-22, Ala-18, and Lys-15 were responsible for the splaying of the coiled coil.

coil, residues in positions *a* and *d* are usually middle-sized and hydrophobic, with a typical example being leucine. At the interface between the two α-helices, these hydrophobic residues at positions *a* and *d* interact with those on the other helix.[113]

Tropomyosin has also a 7-fold sequence repeat,[114] and each motif ($\sim$40 residues) is thought to interact similarly with one actin protomer (monomer). To accommodate its wide range of functions, tropomyosin exists in $\sim$40 isoforms, which are expressed from four genes.[115] Each tropomyosin gene is composed of nine exons. Exons 1, 2, 6, and 9 are alternatively spliced.[116] The COOH-terminal region of tropomyosin anchors troponin-T.[117]

To anchor troponin-T, the COOH-terminal region of tropomyosin has to be encoded by the striated muscle-specific exon 9a.[118)]

Figure 11A shows a schematic model of actin-tropomyosin, together with fragments from the NH- and COOH-terminal regions of tropomyosin chosen for crystallization. Figure 12A shows the 2.1-Å resolution structure of the TM-C:TM-N binary complex.[119)] TM-C fragment contains the COOH-terminal region of tropomyosin, and TM-N fragment contains the NH-terminal region of tropomyosin. In the former, the residues 254–284 of the COOH-terminal region of α-tropomyosin (C-Tm) were preceded by a 20-residue fragment of the GCN4, a transcription factor with the leucine-zipper motif,[120)] to facilitate the formation of coiled-coil structure. In the latter, the residues 1–24 of the NH-terminal region of α-tropomyosin (N-Tm) were followed by a 12-residue fragment of the GCN4, and preceded by NH-terminal Gly-Ala-Ala-Ser extension to mimic acetylation of the NH-terminus required for the head-to-tail interaction.[121),122)]

As shown in Fig. 12A, the residues 254–281(C-Tm) of the TM-C formed a coiled coil as expected. Although the residues 16–36 of TM-N formed a coiled-coil, two α-helices of TM-N were splayed apart from Met-1 to Lys-15 as shown in Figs. 11B and 12. The residues 1–11 interacted with one of the α-helices of TM-C (S-arm, non-kinked α-helix, see below). The interface between TM-C and TM-N was only 165 Å^2 in the binary complex, and is consistent with the weak head-to-tail interaction of skeletal tropomyosin (K_d 10–100 µM).

At the junction between TM-C and TM-N, hydrophobic residues of TM-N α-helix packed against one of TM-C α-helices (S-arm, non-kinked α-helix). The junction showed "knob-in-hole" packing: The hydrophobic side chain of the Leu-278 of the one of TM-C α-helices (S-arm, non-kinked α-helix) was inserted as a "knob" into a hydrophobic "hole" formed by Ile-4, Lys-7, and Met-8 of TM-N. The "hole" is indicated by a dotted triangle in the right panel of Fig. 12A. Interestingly, Leu-278 is conserved (Leu or Phe) between isoforms.

Figure 12B shows the similar "knob-in-hole" packing in the ternary complex of TM-C, TM-N, and TnT (residues 58–112) determined at a 2.9-Å resolution. The hydrophobic "hole" formed by Ile-4, Lys-7, and Met-8 of TM-N is indicated by a dotted triangle in the right panel.

The segment of TnT was chosen to include the highly conserved region (residues 69–112), in which

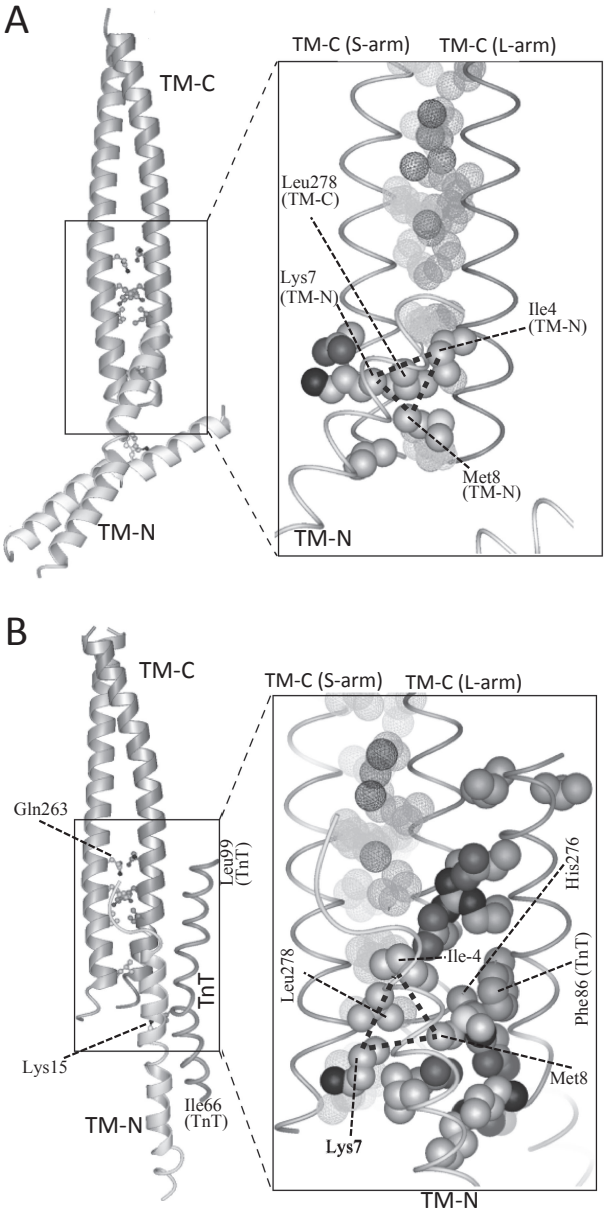

Fig. 12. The atomic structure of tropomyosin junction as determined by X-ray crystallography.[119)] A. TM-C:TM-N binary complex. B. TM-C:TM-N:TnT ternary complex. In both complexes, responsible residues for the formation of tropomyosin junction were the same: Leu-278, Ile-4, Lys-7, and Met-8. The Leu-278 functions as a "knob", which binds to a "hole" formed by Ile-4, Lys-7, and Met-8. The "hole" is indicated by a dotted triangle. The interaction between the "knob" and the "hole" was mainly hydrophobic, and the "knob-in-hole" interaction may work as a "ball-and-socket" joint, in which the ball-shaped "knob" moves smoothly inside a curved hollow "hole". Thus, the "knob-in-hole" interaction may work as an adjustable swivel, which allows the swing of TM-N against TM-C at the junction, and allows to bridge the ~20-Å gap between the azimuthal position of the COOH-terminal one-third and that of the NH-terminal one-half of tropomyosin at low Ca^{2+} concentrations.

many cardiomyopathy mutations are found.[123] It is remarkable that the same residues contributed to the packing as in the binary complex, even though the orientation of TM-N relative to TM-C differed by ~50° in comparison with the binary complex shown in Fig. 12A. This suggests that the "knob-in-hole" interaction may work as a "ball-and-socket" joint such as the hip joint, in which the ball-shaped "knob" moves smoothly inside a curved hollow "hole". Thus, the "knob-in-hole" interaction may work as an adjustable swivel, which allows the swing of TM-N against TM-C at the junction. Without the swivel action, it would be difficult to bridge the ~20-Å gap between the azimuthal position of the COOH-terminal one-third and that of the NH-terminal one-half of tropomyosin at low Ca^{2+} concentrations. The hydrophobic interaction also plays a role of lubricant for the smooth movement of a "ball-and-socket" joint.

The arrangement shown in Fig. 12 differed from that in an NMR structure, in which the COOH-termini instead of the NH-termini splayed apart.[124] The main origin of the inconsistency between our X-ray structure and the NMR structure[124] may be the difference in the peptide design of the NH-terminal fragment (TM-N). The latter[124] contained the residues 1–14, and lacks residues 15, 18, and 22, which play, as described below, a key role in destabilizing a coiled coil: The combination of too large side chain (Lys-15 in position *a*) and too small side chains (Ala-18 and Ala-22 in positions *d* and *a*, respectively) is unfavorable for the stable coiled-coil structure. Thus, the replacement of residues 15–24 with the GCN4 sequence, which is a powerful former of a coiled-coil structure, would hinder the splaying of the coiled coil in NH-terminal region.

The crystal structures of TM-C without TM-N also showed the splayed COOH-termini.[125),126] In the TM-C:TM-N binary complex from chicken smooth muscle, the COOH-terminal helices also splayed apart.[127] These results suggest the flexibility of the terminal regions of tropomyosin, and the COOH-termini can take up many conformations including a splayed one. From a physiological viewpoint, however, a caveat is that all of these results including ours were obtained using fragments of tropomyosin.

Therefore, the binding of full-length tropomyosin with actin filaments was examined. Two lines of evidence suggest that the NH-terminal splaying is important for skeletal tropomyosin to bind to actin filaments. Firstly, three conserved residues (Lys-15, Ala-18, Ala-22), which were either too large or too small to stabilize coiled coil, were mutated to leucine, which stabilizes the canonical coiled coil. This mutant tropomyosin showed almost no actin binding. Secondly, Met-1 at the NH-terminal region was mutated to cysteine and mildly air-oxidized to form disulfide bond between two tropomyosin α-helices and to prevent the splaying. Actin binding of the resultant tropomyosin markedly decreased, but the binding capability could be rescued by reducing the disulfide bond with dithiothreitol. The control experiments using the Ile284-to-Cys mutant tropomyosin to crosslink the COOH-termini showed that the effect on actin binding was much milder.

6.2. Interaction of troponin-T with tropomyosin junction. Figure 12B shows that the part of TnT (residues 66–99) helps stabilize the junction by interacting with both of the TM-C and the TM-N. The interaction between TnT and the tropomyosin junction was in an antiparallel orientation that was consistent with the crystal structure of tropomyosin-troponin.[117]

Interacting residues of TnT coincided with the highly conserved region (residues 69–112), in which many cardiomyopathy mutations were reported. In particular, the planar side chain of Phe-86 of TnT faced against that of His-276 of TM-C (L-arm) as shown in Figs. 13B and 14: The Phe-86 corresponds to cardiac Phe-110, of which the mutation causes hypertrophic cardiomyopathy. *In vitro* experiments showed that Phe86-to-Ile mutation introduced to TnT weakened the interaction of troponin with actin-tropomyosin.[123]

6.3. Asymmetry of the tropomyosin coiled coil. The TM-C used for crystallography was a parallel homo-dimer and two α-helices are expected to form a symmetric coiled-coil structure. However, either in the absence (Fig. 13A) or presence of TnT (Figs. 13B–C), one α-helix (L-arm) was more bent and followed a longer path than the other (S-arm). The L-arm of TM-C was markedly kinked. The S-arm was almost parallel to the L-arm in the region including residues 263–270, and a steric clash at the interface between two α-helices was avoided. The kink was observed near Ile-270 at the end of the parallel region.

Figure 13A shows that the asymmetry was augmented by the cation-π interaction[128] between positively charged ε-amino group of Lys-266 (S-arm) and Tyr-267 (L-arm), of which the phenol ring contains many π-electrons. Two water molecules formed the hydrogen bond with Gln-263 and labeled as WAT1 and WAT2. One of them (WAT1) is unusual, because it was located in the hydrophobic

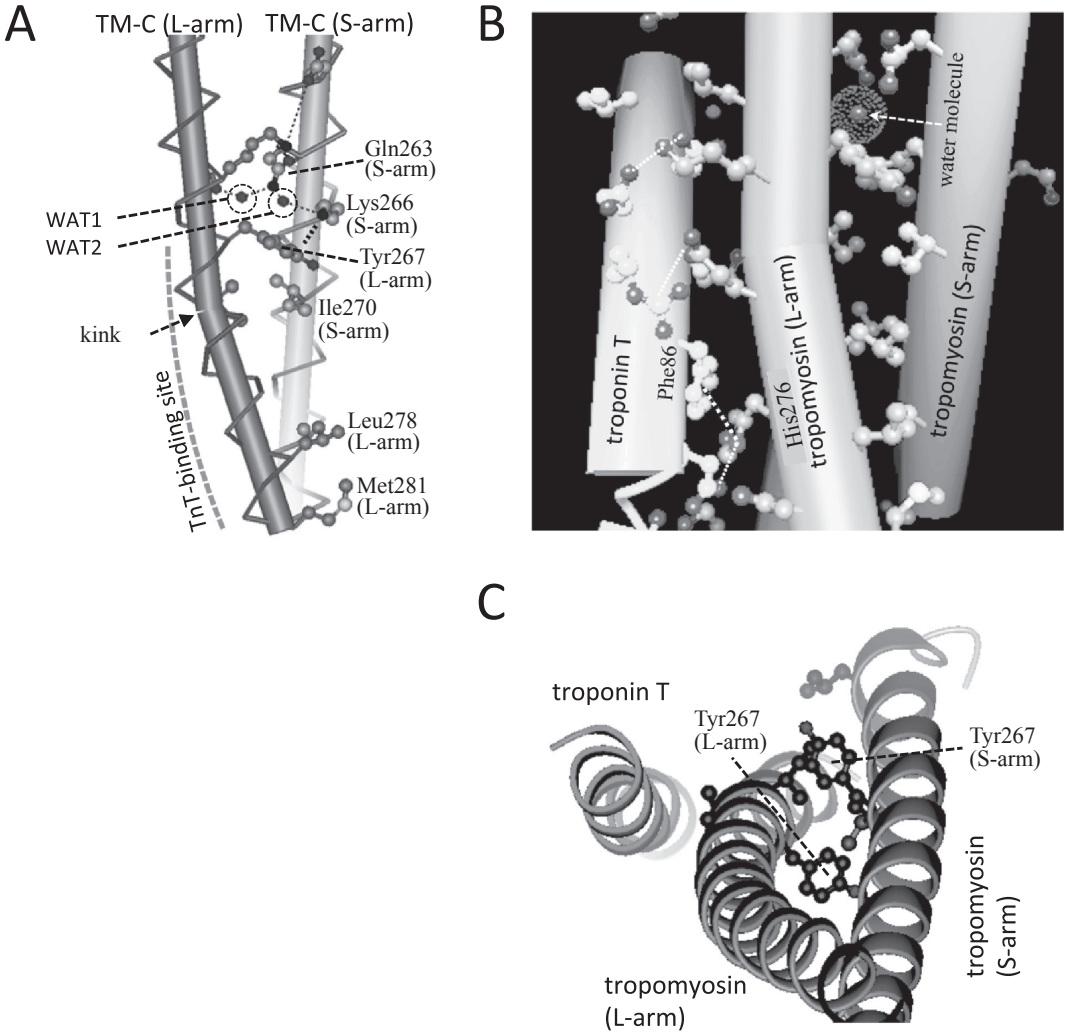

Fig. 13. Asymmetry of the tropomyosin coiled coil as determined by X-ray crystallograpy.[119] A. In a coiled-coil structure of COOH-region of tropomyosin in the binary complex, one of α-helix (L-arm) was kinked. One water molecule in the hydrophobic core facilitated asymmetry and labeled as WAT1, whereas the other water molecule is labeled as WAT2. B. Troponin-T binds to the kinked region of L-arm. The water molecule in the hydrophobic core was also observed in the ternary complex. The planar side chain of His-276 of TM-C (L-arm) face against that of Phe-86 (cardiac Phe-110) of TnT. C. The top view from the M-line side. Two Tyr-267s of L-arm and S-arm near the hydrophobic core responsible for the kink formation are shown in ball-and-stick format.

core of a coiled-coil structure. This water molecule helped break the symmetry between two α-helices, because it cannot be equally shared by two α-helices.

The asymmetry of two α-helices and the kink were crucial to form the head-to-tail junction, because the side chain of Met-281 of the L-arm folded back onto the Leu-278 of L-arm, and the latter cannot function as a "knob" to interact with TM-N as shown in Fig. 13A. On the other hand, the Leu-278 of S-arm was free to bind TM-N. The residues responsible for the kink shown in Fig. 13A are conserved only in striated-muscle tropomyosins (residues 263 (Gln or Glu), 266 (Lys or Arg), 267 (Tyr), and 270 (Ile)). This suggests that the asymmetric structure of the COOH-terminal region may be striated-muscle specific and is required to anchor TnT.

Figures 13B and 13C show a side view and a top view of the TM-C:TM-N:TnT ternary complex, respectively. The L-arm of TM-C in the ternary complex also showed the similar kink to that in the binary complex. The unusual water molecule was also observed in the hydrophobic core of the coiled-coil structure. It suggests that the unusual water molecule is one of the important components to generate asymmetry. The kink appeared to be essential for TnT binding, because it allowed close

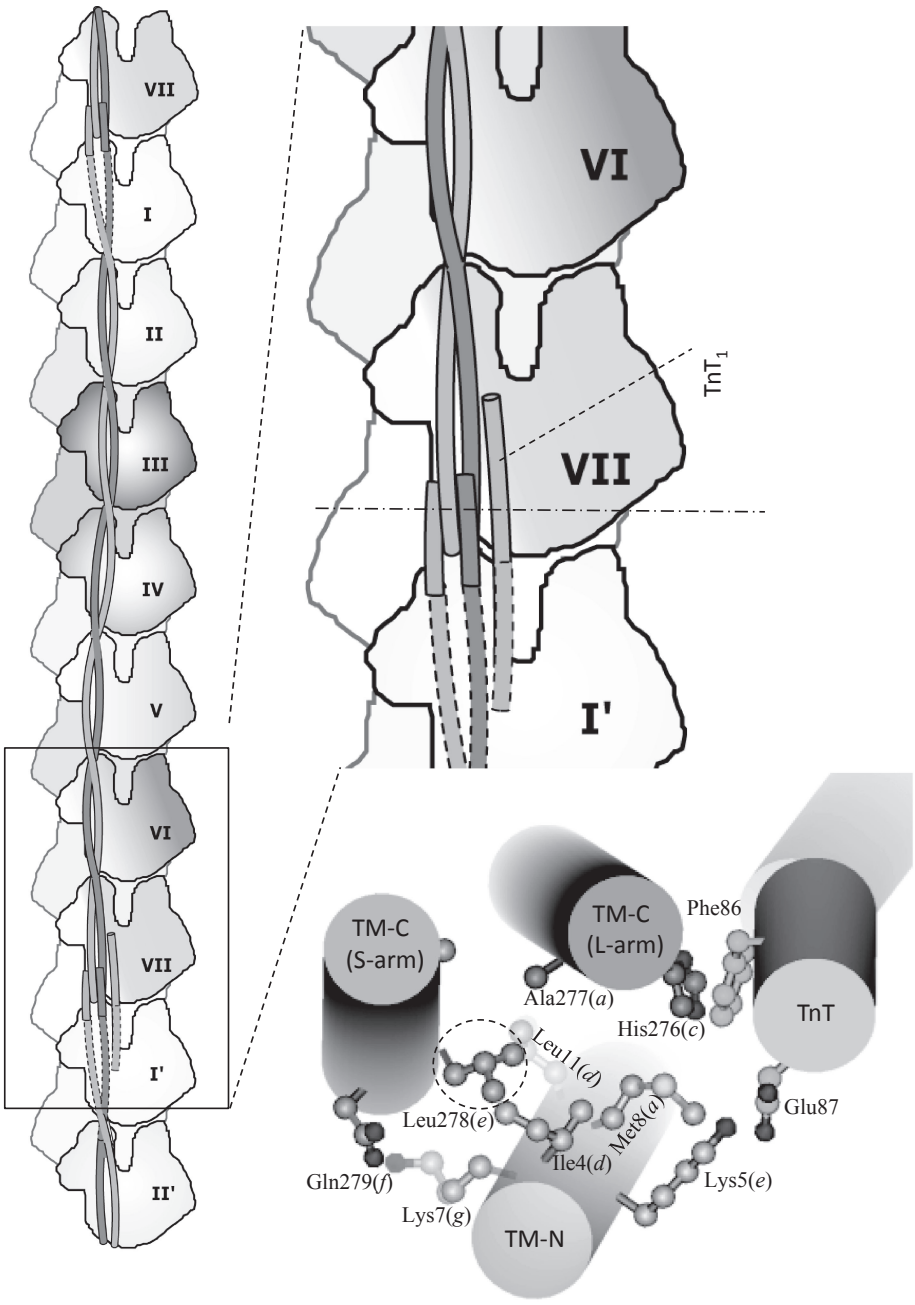

Fig. 14. Four-helix bundle formed by troponin-T and tropomyosin junction as determined by X-ray crystallography of the ternary complex of TM-C, TM-N and TnT.[119] Troponin-T and the tropomyosin junction formed an asymmetric four-helix bundle. The cylinder model is viewed from the M-line side. It also shows the "knob" (Leu-278 of TM-C), which is encircled, surrounded by hydrophobic side chains of Ile-4, Met-8, Leu-11, and the aliphatic part of Lys-7 of TM-N. The side chain of Phe-86 (cardiac Phe-110) of TnT faced against that of His-276 of TM-C (L-arm). This interaction is important to prevent the human cardiomyopathy.[123]

packing between the kinked L-arm of TM-C and TnT with the optimal helix-crossing angle of ∼18°. The His276 of kinked L-arm of TM-C faced against the Phe86 of TnT. The asymmetry introduced by the kink in TM-C also explains why homo-dimeric tropomyosin binds only one troponin molecule even in the absence of actin.[129]

6.4. Four-helix bundle formed by tropomyosin and troponin-T. Figure 14 shows schematic drawings and a cylinder model to illustrate how the

tropomyosin junction together with troponin-T formed an asymmetric four-helix bundle, which frequently occurs as domains in proteins rich in α-helices. The cylinder model is viewed from the M-line side. It also shows the "knob" (Leu-278 of TM-C) surrounded by hydrophobic side chains of Ile-4, Met-8, Leu-11, and the aliphatic part of Lys-7 of TM-N. The distance from TnT α-helix to TM-C (L-arm) α-helix was as short as $\sim$9 Å, and the side chain of Phe-86 of TnT faced against that of His-276 of TM-C (L-arm). There is electrostatic interaction between Glu-87 of TnT and Lys-5 of TM-N, but the inter-helix distance was longer ($\sim$15 Å).

6.5. Implications of disruption (splaying) of tropomyosin coiled coil in the junction. The most important feature of the disruption (splaying) of a coiled-coil structure in the NH-terminal region of tropomyosin is that the "hole" generated by Ile-4, Lys-7, and Met-8 can more easily reach the "knob" (Leu-278) at the COOH-terminal region. The "knob-in-hole" interaction works as an adjustable swivel, which by swinging of TM-N against TM-C at the junction allows bridging the gap of the difference in the azimuthal positions of the COOH-terminal region and that of the NH-terminal region of tropomyosin. Thus, tropomyosin can form the "head-to-tail" junction even at the low concentrations of Ca^{2+}, where the differential shift of tropomyosin takes place as described in the section 4.4.

Figure 15 shows schematically three states of actin-tropomyosin-troponin. At high Ca^{2+} concentrations, tropomyosin follows the long-pitch helix of actin filaments and the necessity of the swivel is not apparent. However, at low Ca^{2+} concentrations, the swivel mechanism is required to form a continuous rope by compensating for the difference in the extent of the azimuthal shift. This feature is also important for the equivalent relationship of successive tropomyosin molecules and actin filament.[111),112)]

As shown in Figures 12B and 14, TnT appeared to help break the 2-fold symmetry of the coiled-coil structure by binding only to one of two α-helices of splayed TM-N, and by binding only to the L-arm (kinked α-helix) of TM-C.

7. Proposed structural three-state model for Ca^{2+}-regulation

Figure 15 shows the proposed structural three-state model for Ca^{2+}-regulation.[84)] At high Ca^{2+} (right two panels), there are two states, with a T-state (or "closed" state) being $\sim$10 times higher in population than an R-state (or "open" state) in the absence of the interaction with myosin as proposed on the basis of biochemical data.[130),131)] Therefore, the structure at high Ca^{2+} described in the section 4 and shown in Figs. 7–8 represents that in a "closed" T-state, in which actin-tropomyosin-troponin cannot fully activate myosin ATPase. When myosin interacts with the actin-tropomyosin-troponin in a T-state, the T-to-R transition takes place so that an R-state becomes much higher in population than a T-state so that the interaction between actin and myosin is fully activated. Because of the presence of myosin S1 in the actin-tropomyosin-myosin S1-ADP-Vi complex shown in Figs. 6A and 6D, the complex represents that in an "open" R-state. The position of tropomyosin is near to Ala-230 of actin, of which the mutation to tyrosine induced higher Ca^{2+}-activation in the presence of tropomyosin and troponin.[132)–134)] Presumably the Ala-to-Tyr mutation would favor the R-state position of tropomyosin so that myosin can more readily interact with actin-tropomyosin-troponin.

The structure at low Ca^{2+} (apo-state, left panel of Fig. 15) shown in the left panels of Figs. 7–8 represents a "blocked" T*-state, in which the tight interaction between the troponin arm (mobile domain) and the COOH-terminal region of actin causes the shift of the COOH-terminal one-third of tropomyosin but not that of the NH-terminal one-half resulting in the differential shift of tropomyosin. The swivel formed at the tropomyosin junction can bridge the gap in the azimuthal positions between the more shifted COOH-terminal region and the less shifted NH-terminal region.

The differential shift of troponin can explain why the inhibition at low Ca^{2+} is not so perfect as that of myosin-regulated smooth muscles, because the extent of the tropomyosin shift in NH-terminal region was not large enough to completely block the myosin binding.[84)]

Acknowledgements

The author extends thanks to Drs. Yasuo Shirakihara, Chikashi Toyoshima, Akihiro Tomioka, Eisaku Katayama, Masashi Suzuki, Keiko Hirose, Toshihiko Akiba, Takao Matsumoto, Ken-ichiro Mogi, Makio Tokunaga, Takuo Yasunaga, Shigehiro Nagashima, Takashi Ishikawa, Masahide Kikkawa, Hisashi Yamakawa, Yu Meng, Kouta Mayanagi, Shuhei Hashiba, Yoshiyuki Matsuura, Kaoru Mitsuoka, Akihiro Narita, Kenji Murakami, Kimiko Saeki, with whom he has worked in the Department of Physics, School of Science, the University of

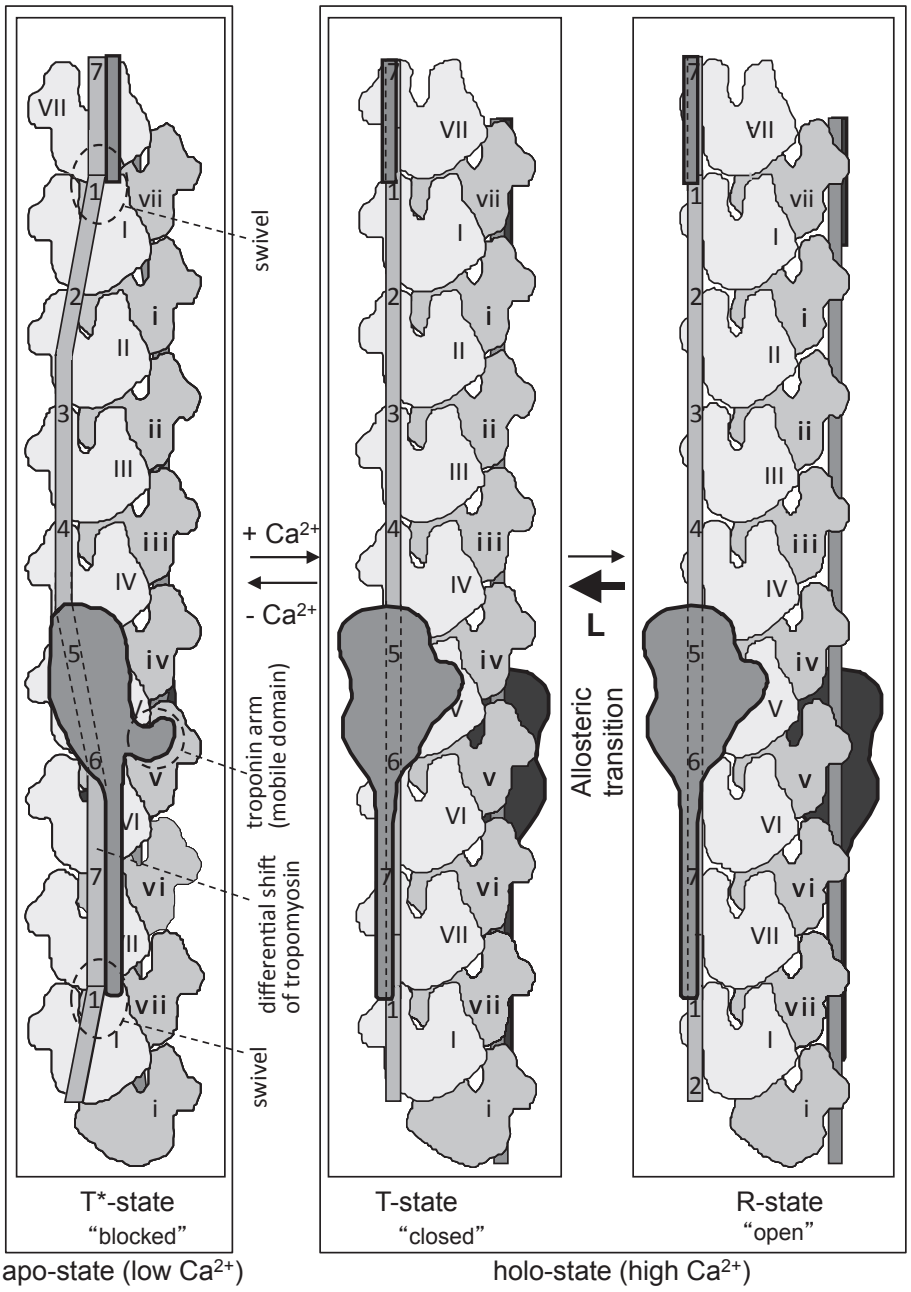

Fig. 15. Proposed structural three-state model for Ca^{2+}-regulation.[84] To simplify the illustrations, actin helix was untwisted so that two strands become parallel. At low Ca^{2+} ("blocked" T* state), the swivel[119] formed by tropomyosin junction and troponin-T compensate for the differential shift[84] of tropomyosin induced by the tight association of the troponin arm[84] with actin. The differential shift can explain why the inhibition at low Ca^{2+} is not perfect. At high Ca^{2+} (holo-state), there are two states, a "closed" T-state and an "open" R-state as proposed on the basis of biochemical data.[130),131] The structure at high Ca^{2+} shown in the right panel of Fig. 7A represents a "closed" T-state, whereas the position of tropomyosin in the actin-tropomyosin-myosin S1-ADP-Vi complex shown in Figs. 6A and 6D[55] is located nearer to the groove of actin double helix and represents that in an "open" R-state, because the binding of myosin induces the "close"-to-"open" transition. This position is near to Ala-230 of actin, of which the mutation to tyrosine induced higher Ca^{2+}-activation in the presence of tropomyosin and troponin, which is an important feature of the "open" R-state.[132)–134)]

Tokyo, and Dr. Yuki Gomibuchi, with whom he has been working in the Department of Biosciences, School of Science and Engineering, Teikyo University. The author thanks Drs. Kazuo Sutoh, Murray Stewart, Katsuzo Wakabayashi, Fumiaki Yumoto, Shin-ya Ohki, and Masaru Tanokura for their kind collaboration. The author would like to thank late Prof. Setsuro Ebashi, late Prof. Hugh E. Huxley, and Dr. Aaron Klug for their patient mentorship. The work was supported by the grants from the Ministry of Education, Science, Culture and Sports, Science and Technology of Japan, the Institute of Physical Chemical Research (RIKEN), the HFSP (Human Frontier Science Foundation), the Mitsubishi Foundation, and the Toray Science Foundation.

References

1) Straub, F.B. (1942) Actin. Studies Int. Med. Chem. Univ. Szeged **2**, 3–15.
2) Szent-Gyorgyi, A. (1951) Chemistry of Muscular Contraction, 2nd ed., Academic Press, New York, NY.
3) Wegner, A. (1976) Head to tail polymerization of actin. J. Mol. Biol. **108**, 139–150.
4) Fujiwara, I., Takahashi, S., Tadakuma, H., Funatsu, T. and Ishiwata, S. (2002) Microscopic analysis of polymerization dynamics with individual actin filaments. Nat. Cell Biol. **4**, 666–673.
5) Matus, A. (1999) Postsynaptic actin and neuronal plasticity. Curr. Opin. Neurobiol. **9**, 561–565.
6) Hirono, M., Endoh, H., Okada, N., Numata, O. and Watanabe, Y. (1987) *Tetrahymena* actin. Cloning and sequencing of the *Tetrahymena* actin gene and identification of its gene product. J. Mol. Biol. **194**, 181–192.
7) Ohtsuki, I. and Wakabayashi, T. (1972) Optical diffraction studies on the structure of troponin-tropomyosin actin paracrystals. J. Biochem. **72**, 369–377.
8) Ebashi, S. and Kodama, A. (1965) A new protein factor promoting aggregation of tropomyosin. J. Biochem. **58**, 107–108.
9) Greaser, M.L. and Gergely, J. (1971) Reconstruction of troponin activity from three protein components. J. Biol. Chem. **246**, 4226–4233.
10) Ebashi, S. (1972) Separation of troponin into its three components. J. Biochem. **72**, 787–790.
11) Ebashi, S., Wakabayashi, T. and Ebashi, F. (1971) Troponin and its components. J. Biochem. **69**, 441–445.
12) Schaub, M.C. and Perry, S.V. (1969) The relaxing protein system of striated muscle. Resolution of the troponin complex into inhibitory and calcium ion-sensitizing factors and their relationship to tropomyosin. Biochem. J. **115**, 993–1004.
13) Hartshorne, D.J. and Mueller, H. (1968) Fractionation of troponin into two distinct proteins. Biochem. Biophys. Res. Commun. **31**, 647–653.
14) Hanson, J. and Lowy, J. (1963) The structure of F-actin and of actin filaments isolated from muscle. J. Mol. Biol. **6**, 46–60.
15) Depue, R.H. and Rice, R.V. (1965) F-actin is a right-handed helix. J. Mol. Biol. **12**, 302–303.
16) DeRosier, D.J. and Moore, P.B. (1970) Reconstruction of three-dimensional images from electron micrographs of structures with helical symmetry. J. Mol. Biol. **52**, 355–369.
17) Moore, P.B., Huxley, H.E. and De Rosier, D.J. (1970) Three-dimensional reconstructions of F-actin, thin filaments and decorated thin filaments. J. Mol. Biol. **50**, 279–295.
18) Ebashi, S. and Endo, M. (1968) Calcium ion and muscle contraction. Prog. Biophys. Mol. Biol. **18**, 123–183.
19) Ebashi, S., Ebashi, F. and Kodama, A. (1967) Troponin as the Ca^{++}-receptive protein in the contractile system. J. Biochem. **62**, 137–138.
20) Wakabayashi, T. and Ebashi, S. (1968) Reversible change in physical state of troponin induced by calcium ion. J. Biochem. **64**, 731–732.
21) Masaki, T., Wakabayashi, T. and Takaiti, O. (1969) Molecular biology of muscle contraction III —Myofibrillar proteins (2) regulatory proteins—. KAGAKU **39**, 268–274.
22) Ebashi, S., Endo, M. and Ohtsuki, I. (1969) Control of muscle contraction. Q. Rev. Biophys. **2**, 351–384.
23) Wakabayashi, T. (1970) Physicochemical characterization of Ca^{2+}-induced changes of troponin from skeletal muscle, Ph.D. thesis, the University of Tokyo.
24) Ebashi, S. (1972) Calcium ions and muscle contraction. Nature **240**, 217–218.
25) Ohtsuki, I. (1974) Localization of troponin in thin filament and tropomyosin paracrystal. J. Biochem. **75**, 753–765.
26) Ohtsuki, I., Masaki, T., Nonomura, Y. and Ebashi, S. (1967) Periodic distribution of troponin along the thin filament. J. Biochem. **61**, 817–819.
27) Spudich, J.A. and Watt, S. (1971) The regulation of rabbit skeletal muscle contraction. I. Biochemical studies of the interaction of the tropomyosin-troponin complex with actin and the proteolytic fragments of myosin. J. Biol. Chem. **246**, 4866–4871.
28) Nonomura, Y., Drabikowski, W. and Ebashi, S. (1968) The localization of troponin in tropomyosin paracrystals. J. Biochem. **64**, 419–422.
29) Stewart, M. and McLachlan, A.D. (1975) 14 actin binding sites on tropomyosin? Nature **257**, 331–333.
30) Huxley, H.E. (1972) Structural changes in the actin- and myosin-containing filaments during contraction. Cold Spring Harb. Symp. Quant. Biol. **37**, 361–376.
31) Haselgrove, J.C. (1972) X-ray evidence for a conformational change in the actin-containing filaments of vertebrate striated muscle. Cold Spring Harb. Symp. Quant. Biol. **37**, 341–352.
32) Parry, D.A.D. and Squire, J.M. (1973) Structural

role of tropomyosin in muscle regulation: analysis of the X-ray diffraction patterns from relaxed and contracting muscles. J. Mol. Biol. **75**, 33–55.
33) Spudich, J.A., Huxley, H.E. and Finch, J.T. (1972) Regulation of skeletal muscle contraction. II. Structural studies of the interaction of the tropomyosin-troponin complex with actin. J. Mol. Biol. **72**, 619–632.
34) Wakabayashi, T., Huxley, H.E., Amos, L.A. and Klug, A. (1975) Three-dimensional image reconstruction of actin-tropomyosin complex and actin-tropomyosin-troponinT-troponin I complex. J. Mol. Biol. **93**, 477–497.
35) Ishiwata, S. and Fujime, S. (1972) Effect of calcium ions on the flexibility of reconstituted thin filaments of muscle studied by quasi-elastic scattering of laser light. J. Mol. Biol. **68**, 511–522.
36) Amos, L.A. and Klug, A. (1975) Three-dimensional image reconstructions of the contractile tail of T4 bacteriophage. J. Mol. Biol. **99**, 51–64.
37) Huxley, H.E. (1963) Electron microscope studies on the structure of natural and synthetic filaments from striated muscle. J. Mol. Biol. **7**, 281–308.
38) Howling, D.H. and Fitzgerald, P.J. (1959) The nature, significance, and evaluation of the Schwarzschild-Villiger (SV) effect in photometric procedures. J. Biophys. Biochem. Cytol. **6**, 313–337.
39) Toyoshima, C. and Wakabayashi, T. (1985) Three-dimensional image analysis of the complex of thin filaments and myosin molecules from skeletal muscle. IV. Reconstitution from minimal- and high-dose image of the actin-tropomyosin-myosin subfragment-1 complex. J. Biochem. **97**, 219–243.
40) Taylor, K.A. and Amos, L.A. (1981) A new model for the geometry of the binding of myosin cross-bridges to muscle thin filaments. J. Mol. Biol. **147**, 297–324.
41) Wakabayashi, T. and Toyoshima, C. (1981) Three-dimensional image analysis of the complex of thin filaments and myosin molecules from skeletal muscle. II. The multi-domain structure of actin-myosin S1 complex. J. Biochem. **90**, 683–703.
42) Amos, L.A., Huxley, H.E., Holmes, K.C., Goody, R.S. and Taylor, K.A. (1982) Structural evidence that myosin heads may interact with two sites on F-actin. Nature **299**, 467–469.
43) Tomioka, A., Ribi, H.O., Tokunaga, M., Furuno, T., Sasabe, H., Miyano, K. and Wakabayashi, T. (1991) Structural analysis of muscle thin filament. Adv. Biophys. **27**, 169–183.
44) Toyoshima, C. and Wakabayashi, T. (1985) Three-dimensional image analysis of the complex of thin filaments and myosin molecules from skeletal muscle. V. Assignment of actin in the actin-tropomyosin-myosin subfragment-1 complex. J. Biochem. **97**, 245–263.
45) Milligan, R.A. and Flicker, P.F. (1987) Structural relationships of actin, myosin, and tropomyosin revealed by cryo-electron microscopy. J. Cell Biol. **105**, 29–39.
46) Murakami, K., Yasunaga, T., Noguchi, T.Q.P., Gomibuchi, Y., Ngo, K.X., Uyeda, T.Q.P. and Wakabayashi, T. (2010) Structural basis for actin assembly, activation of ATP hydrolysis, and delayed phosphate release. Cell **143**, 275–287.
47) Fujii, T., Iwane, A.H., Yanagida, T. and Namba, K. (2010) Direct visualization of secondary structures of F-actin by electron cryomicroscopy. Nature **467**, 724–728.
48) Galkin, V.E., Orlova, A., Schroder, G.F. and Egelman, E.H. (2010) Structural polymorphism in F-actin. Nat. Struct. Mol. Biol. **17**, 1318–1323.
49) Behrmann, E., Muller, M., Penczek, P.A., Mannherz, H.G., Manstein, D.J. and Raunser, S. (2012) Structure of the rigor actin-tropomyosin-myosin complex. Cell **150**, 327–338.
50) Kabsch, W., Mannherz, H.G., Suck, D., Pai, E.F. and Holmes, K.C. (1990) Atomic structure of the actin:DNase I complex. Nature **347**, 37–44.
51) Rayment, I., Rypniewski, W.R., Schmidt-Base, K., Smith, R., Tomchick, D.R., Benning, M.M., Winkelmann, D.A., Wesenberg, G. and Holden, H.M. (1993) Three-dimensional structure of myosin subfragment-1: a molecular motor. Science **261**, 50–58.
52) Rayment, I., Holden, H.M., Whittaker, M., Yohn, C.B., Lorenz, M., Holmes, K.C. and Millgan, R.A. (1993) Structure of the actin-myosin complex and its implications for muscle contraction. Science **261**, 58–65.
53) Sutoh, K., Yamamoto, K. and Wakabayashi, T. (1984) Electron microscopic visualization of SH1 thiol of myosin by the use of an avidin-biotin system. J. Mol. Biol. **178**, 323–339.
54) Sutoh, K., Yamamoto, K. and Wakabayashi, T. (1986) Electron microscopic visualization of the ATPase site of myosin by the use of a biotinylated photo-affinity ADP analog. Proc. Natl. Acad. Sci. U.S.A. **83**, 212–216.
55) Tokunaga, M., Sutoh, K., Toyoshima, C. and Wakabayashi, T. (1987) Location of the ATPase site of myosin determined by three-dimensional electron microscopy. Nature **329**, 635–638.
56) Huxley, H.E. (1969) The mechanism of muscular contraction. Science **164**, 1356–1366.
57) Toyoshima, C. and Wakabayashi, T. (1979) Three-dimensional image analysis of the complex of thin filaments and myosin molecules from skeletal muscle. I. Tilt angle of myosin subfragment-1 in rigor complex. J. Biochem. **86**, 1887–1890.
58) Yagi, N., O'Brien, E.J. and Matsubara, I. (1981) Changes of thick filament structure during contraction of frog striated muscle. Biophys. J. **33**, 121–138.
59) Yanagida, T. (1981) Angles of nucleotides bound to cross-bridges in glycerinated muscle fiber at various concentrations of ε-ATP, ε-ADP and ε-AMPPNP detected by polarized fluorescence. J. Mol. Biol. **146**, 539–560.
60) Huxley, H.E., Faruqi, A.R., Kress, M., Bordas, J. and Koch, M.H.J. (1982) Time-resolved X-ray diffraction studies of the myosin layer-line reflections during muscle contraction. J. Mol. Biol. **158**,

637–684.
61) Cooke, R., Crowder, M.S. and Thomas, D.D. (1982) Orientation of spin labels attached to cross-bridges in contracting muscle fibres. Nature **300**, 776–778.
62) Borejdo, J., Assulin, O., Ando, T. and Putnam, S. (1982) Cross-bridge orientation in skeletal muscle measured by linear dichroism of an extrinsic chromophore. J. Mol. Biol. **158**, 391–414.
63) Winkelmann, D.A., Mekeel, H. and Rayment, I. (1985) Packing analysis of crystalline myosin subfragment-1: Implications for the size and shape of the myosin head. J. Mol. Biol. **181**, 487–501.
64) Tokunaga, M., Sutoh, K. and Wakabayashi, T. (1991) Structure and structural change of the myosin head. Adv. Biophys. **27**, 157–167.
65) Wakabayashi, K., Tokunaga, M., Kohno, I., Sugimoto, Y., Hamanaka, T., Takezawa, Y., Wakabayashi, T. and Amemiya, Y. (1992) Small-angle synchrotron x-ray scattering reveals distinct shape changes of the myosin head during hydrolysis of ATP. Science **258**, 443–447.
66) Suzuki, Y., Yasunaga, T., Ohkura, R., Wakabayashi, T. and Sutoh, K. (1998) Swing of the lever arm of a myosin motor at the isomerization and phosphate-release steps. Nature **396**, 380–383.
67) Werber, M.M., Peyser, Y.M. and Muhlrad, M. (1992) Characterization of stable beryllium fluoride, aluminum fluoride, and vanadate containing myosin subfragment 1-nucleotide complexes. Biochemistry **31**, 7190–7197.
68) Smith, C.A. and Rayment, I. (1996) X-ray structure of the magnesium(II)·ADP·vanadate complex of the *Dictyostelium discoideum* myosin motor domain to 1.9 Å resolution. Biochemistry **35**, 5404–5417.
69) Gulick, A.M., Bauer, C.B., Thoden, J.B. and Rayment, I. (1997) X-ray structures of the MgADP, MgATPγS, and MgAMPPNP complexes of the *Dictyostelium discoideum* myosin motor domain. Biochemistry **36**, 11619–11628.
70) Yasunaga, T., Suzuki, Y., Ohkura, R., Sutoh, K. and Wakabayashi, T. (2000) ATP-induced transconformation of myosin revealed by determining three-dimensional positions of fluorophores from fluorescence energy transfer measurements. J. Struct. Biol. **132**, 6–18.
71) Dobbie, I., Linari, M., Piazzesi, G., Reconditi, M., Koubassova, N., Ferenczi, M.A., Lombardi, V. and Irving, M. (1998) Elastic bending and active tilting of myosin heads during muscle contraction. Nature **396**, 383–387.
72) Endo, M. (1977) Calcium release from the sarcoplasmic reticulum. Physiol. Rev. **57**, 71–108.
73) Lehman, W., Craig, R. and Vibert, P. (1994) Ca^{2+}-induced tropomyosin movement in limulus thin filaments revealed by three-dimensional reconstruction. Nature **368**, 65–67.
74) Lehman, W., Vibert, P., Uman, P. and Craig, R. (1995) Steric-blocking by tropomyosin visualized in relaxed vertebrate muscle thin filaments. J. Mol. Biol. **251**, 191–196.
75) Ishikawa, T. and Wakabayashi, T. (1994) Calcium induced change in three-dimensional structure of thin filaments of rabbit skeletal muscle as revealed by cryoelectron microscopy. Biochem. Biophys. Res. Commun. **203**, 951–958.
76) Vibert, P., Craig, R. and Lehman, W. (1997) Steric-model for activation of muscle thin filaments. J. Mol. Biol. **266**, 8–14.
77) Xu, C., Craig, R., Tobacman, L., Horowitz, R. and Lehman, W. (1999) Tropomyosin positions in regulated thin filaments revealed by cryoelectron microscopy. Biophys. J. **77**, 985–992.
78) Squire, J.M. and Morris, E.P. (1998) A new look at thin filament regulation in vertebrate skeletal muscle. FASEB J. **12**, 761–771.
79) Ishikawa, T. and Wakabayashi, T. (1999) Calcium-induced changes in the location and conformation of troponin in skeletal muscle thin filaments. J. Biochem. **126**, 200–211.
80) Frank, J. (1996) Three-Dimensional Electron Microscopy of Macromolecular Assemblies. Academic Press, San Diego, CA.
81) Frank, J. and Radermacher, M. (1992) Three-dimensional reconstruction of single particles negatively stained or in vitreous ice. Ultramicroscopy **46**, 241–262.
82) van Heel, M. (1987) Angular reconstitution: a posteriori assignment of projection directions for 3D reconstruction. Ultramicroscopy **21**, 111–123.
83) Dubochet, J., Adrian, M., Chang, J.-J., Homo, J.-C., Lepault, J., McDowall, A.W. and Schultz, P. (1988) Cryo-electron microscopy of vitrified specimens. Q. Rev. Biophys. **21**, 129–228.
84) Narita, A., Yasunaga, T., Ishikawa, T., Mayanagi, K. and Wakabayashi, T. (2001) Ca^{2+}-induced switching of troponin and tropomyosin on actin filaments as revealed by electron cryo-microscopy. J. Mol. Biol. **308**, 241–261.
85) Wray, J., Vibert, P. and Cohen, C. (1978) Actin filaments in muscle: Pattern of myosin and tropomyosin/troponin attachments. J. Mol. Biol. **124**, 501–521.
86) Maéda, Y. (1979) X-ray diffraction patterns from molecular arrangements with 38-nm periodicities around muscle thin filaments. Nature **277**, 670–672.
87) Maéda, Y., Matsubara, I. and Yagi, N. (1979) Structural changes in thin filaments of crab striated muscle. J. Mol. Biol. **127**, 191–201.
88) Namba, K., Wakabayashi, K. and Mitsui, T. (1980) X-ray structure analysis of the thin filament of crab striated muscle in the rigor state. J. Mol. Biol. **138**, 1–26.
89) Milligan, R.A. (1996) Protein-protein interactions in the rigor actomyosin complex. Proc. Natl. Acad. Sci. U.S.A. **93**, 21–26.
90) Kimura, C., Maeda, K., Maéda, Y. and Miki, M. (2002) Ca^{2+}- and S1-induced movement of troponin T on reconstituted skeletal muscle thin filaments observed by fluorescence energy transfer spectroscopy. J. Biochem. **132**, 93–102.

91) Kress, M., Huxley, H.E., Faruqi, A.R. and Hendrix, J. (1986) Structural changes during activation of frog muscle studied by time-resolved X-ray diffraction. J. Mol. Biol. **188**, 325–342.
92) Takeda, S., Yamashita, A., Maeda, K. and Maéda, Y. (2003) Structure of the core domain of human cardiac troponin in the Ca^{2+}-saturated form. Nature **424**, 35–41.
93) Miki, M., Miura, T., Sano, K.-I., Kimura, H., Kondo, H., Ishida, H. and Maéda, Y. (1998) Fluorescence resonance energy transfer between points on tropomyosin and actin in skeletal muscle thin filaments: does tropomyosin move? J. Biochem. **123**, 1104–1111.
94) Miki, M., Kobayashi, T., Kimura, H., Hagiwara, A., Hai, H. and Maéda, Y. (1998) Ca^{2+}-induced distance change between points on actin and troponin in skeletal muscle thin filaments estimated by fluorescence energy transfer spectroscopy. J. Biochem. **123**, 324–331.
95) Miki, M., Hai, H., Saeki, K., Shitaka, Y., Sano, K., Maéda, Y. and Wakabayashi, T. (2004) Fluorescence resonance energy transfer between points on actin and the C-terminal region of tropomyosin in skeletal muscle thin filaments. J. Biochem. **136**, 39–47.
96) Maytum, R., Lehrer, S.S. and Geeves, M.A. (1999) Cooperativity and switching within the three-state model of muscle regulation. Biochemistry **38**, 1102–1110.
97) Shimizu, H., Fujita, T. and Ishiwata, S. (1992) Regulation of tension development by MgADP and Pi without Ca^{2+}. Role in spontaneous tension oscillation of skeletal muscle. Biophys. J. **61**, 1087–1096.
98) Farah, C.S., Miyamoto, C.A., Ramos, C.H.I., Dasilva, A.C.R., Quaggio, R.B., Fujimori, K., Smillie, L.B. and Reinach, F.C. (1994) Structural and regulatory functions of the NH- and COOH-terminal regions of skeletal-muscle troponin-I. J. Biol. Chem. **269**, 5230–5240.
99) Rarick, H.M., Tu, X.H., Solaro, R.J. and Martin, A.F. (1997) The C terminus of cardiac troponin I is essential for full inhibitory activity and Ca^{2+} sensitivity of rat myofibrils. J. Biol. Chem. **272**, 26887–26892.
100) Tripet, B., Van Eyk, J.E. and Hodges, R.S. (1997) Mapping of a second actin-tropomyosin and a second troponin C binding site within the C terminus of troponin I, and their importance in the Ca^{2+}-dependent regulation of muscle contraction. J. Mol. Biol. **271**, 728–750.
101) Ramos, C.H.I. (1999) Mapping subdomains in the C-terminal region of troponin I involved in its binding to troponin C and to thin filament. J. Biol. Chem. **274**, 18189–18195.
102) Murakami, K., Yumoto, F., Ohki, S., Yasunaga, T., Tanokura, M. and Wakabayashi, T. (2005) Structural basis for Ca^{2+}-regulated muscle relaxation at interaction sites of troponin with actin and tropomyosin. J. Mol. Biol. **352**, 178–201.
103) Ohtsuki, I. (1979) Molecular arrangement of tropomyosin-T in the thin filament. J. Biochem. **86**, 491–497.
104) Klug, A. and Rhodes, D. (1987) Zinc fingers: a novel protein fold for nucleic acid recognition. Cold Spring Harb. Symp. Quant. Biol. **52**, 473–482.
105) Wakabayashi, T. and Ebashi, S. (2004) Calcium signaling: Motility (actomyosin-troponin system). *In* Encyclopedia of Biological Chemistry (eds. Lennarz, W.J. and Lane, M.D.). Elsevier, Oxford, Vol. 1, pp. 250–255.
106) Gomes, A.V. and Potter, J.D. (2004) Molecular and cellular aspects of troponin cardiomyopathies. Ann. N. Y. Acad. Sci. **1015**, 214–224.
107) DesMarais, V., Ichetovkin, I., Condeelis, J. and Hitchcock-DeGregori, S.E. (2002) Spatial regulation of actin dynamics: a tropomyosin-free, actin-rich compartment at the leading edge. J. Cell Sci. **115**, 4649–4660.
108) Wegner, A. (1982) Kinetic analysis of actin assembly suggests that tropomyosin inhibits spontaneous fragmentation of actin filaments. J. Mol. Biol. **161**, 217–227.
109) Broschat, K.O., Weber, A. and Burgess, D.R. (1989) Tropomyosin stabilizes the pointed end of actin filaments by slowing depolymerization. Biochemistry **28**, 8501–8506.
110) Bernstein, B.W. and Bamburg, J.R. (1982) Tropomyosin binding to F-actin protects the F-actin from disassembly by brain actin-depolymerizing factor (ADF). Cell Motil. **2**, 1–8.
111) Stewart, M. and McLachlan, A.D. (1975) 14 actin binding sites on tropomyosin? Nature **257**, 331–333.
112) McLachlan, A.D. and Stewart, M. (1976) The 14-fold periodicity in α-tropomyosin and interaction with actin. J. Mol. Biol. **103**, 271–298.
113) Crick, F.H.C. (1953) The packing of α-helices: Simple coiled-coils. Acta Crystallogr. **6**, 689–697.
114) McLachlan, A.D. and Stewart, M. (1975) Tropomyosin coiled-coil interactions. J. Mol. Biol. **98**, 293–304.
115) Lees-Miller, J.P. and Helfman, D.M. (1991) The molecular basis for tropomyosin isoform diversity. BioEssays **13**, 429–437.
116) Moraczewska, J., Nicholson-Flynn, K. and Hitchcock-DeGregori, S.E. (1999) The ends of tropomyosin are major determinants of actin affinity and myosin subfragment 1-induced binding to F-actin in the open state. Biochemistry **38**, 15885–15892.
117) White, S.P., Cohen, C. and Phillips, G.N. Jr. (1987) Structure of co-crystals of tropomyosin and troponin. Nature **325**, 826–828.
118) Cho, Y.-J. and Hitchcock-DeGregori, S. (1991) Relationship between alternatively spliced exons and functional domains in tropomyosin. Proc. Natl. Acad. Sci. U.S.A. **88**, 10153–10157.
119) Murakami, K., Stewart, M., Nozawa, K., Tomii, K., Kudou, N., Igarashi, N., Shirakihara, Y., Wakatsuki, S., Yasunaga, T. and Wakabayashi, T. (2008) Structural basis for tropomyosin overlap in thin (actin) filaments and the generation of a

molecular swivel by troponin-T. Proc. Natl. Acad. Sci. U.S.A. **105**, 7200–7205.
120) O'Shea, E.K., Klemm, J.D., Kim, P.S. and Alber, T. (1991) X-ray structure of the GCN4 leucine zipper, a two-stranded, parallel coiled coil. Science **254**, 539–544.
121) Hitchcock-DeGregori, S.E. and Heald, R.W. (1987) Altered actin and troponin binding of amino-terminal variants of chicken striated muscle alpha-tropomyosin expressed in *Escherichia coli*. J. Biol. Chem. **262**, 9730–9735.
122) Monteiro, P.B., Lataro, R.C., Ferro, J.A. and Reinach, F.C. (1994) Functional alpha-tropomyosin produced in *Escherichia coli*. A dipeptide extension can substitute the amino-terminal acetyl group. J. Biol. Chem. **269**, 10461–10466.
123) Hinkle, A. and Tobacman, L.S. (2003) Folding and function of the troponin tail domain. Effects of cardiomyopathic troponin T mutations. J. Biol. Chem. **278**, 506–513.
124) Greenfield, N.J., Huang, Y.J., Swapna, G.V., Bhattacharya, A., Rapp, B., Singh, A., Montelione, G.T. and Hitchcock-DeGregori, S.E. (2006) Solution NMR structure of the junction between tropomyosin molecules: Implications for actin binding and regulation. J. Mol. Biol. **364**, 80–96.
125) Li, Y., Mui, S., Brown, J.H., Strand, J., Reshetnikova, L., Tobacman, L.S. and Cohen, C. (2002) The crystal structure of the C-terminal fragment of striated-muscle α-tropomyosin reveals a key troponin T recognition site. Proc. Natl. Acad. Sci. U.S.A. **99**, 7378–7383.
126) Nitanai, Y., Minakata, S., Maeda, K., Oda, N. and Maéda, Y. (2007) Crystal structures of tropomyosin: Flexible coiled-coil. Adv. Exp. Med. Biol. **592**, 137–151.
127) Frye, J., Klenchin, V.A. and Rayment, I. (2010) Structure of the tropomyosin overlap complex from chicken smooth muscle: Insight into the diversity of N-terminus recognition. Biochemistry **49**, 4908–4920.
128) Gallivan, J.P. and Dougherty, D.A. (1999) Cation-π interaction in structural biology. Proc. Natl. Acad. Sci. U.S.A. **96**, 9459–9464.
129) Pato, M.D., Mak, A.S. and Smillie, L.B. (1981) Fragments of rabbit striated muscle α-tropomyosin. I. Preparation and characterization. J. Biol. Chem. **256**, 593–601.
130) McKillop, D.F.A. and Geeves, M.A. (1993) Regulation of the interaction between actin and myosin subfragment 1: evidence for three states of the thin filament. Biophys. J. **65**, 693–701.
131) Maytum, R., Lehrer, S.S. and Geeves, M.A. (1999) Cooperativity and switching within the three-state model of muscle regulation. Biochemistry **38**, 1102–1110.
132) Saeki, K., Sutoh, K. and Wakabayashi, T. (1996) Tropomyosin-binding site(s) on the *Dictyostelium* actin surface as identified by site-directed mutagenesis. Biochemistry **35**, 14465–14472.
133) Saeki, K. and Wakabayashi, T. (2000) A230Y mutation of actin on subdomain 4 is sufficient for higher calcium activation of actin-activated myosin adenosinetriphosphatase in the presence of tropomyosin-troponin. Biochemistry **39**, 1324–1329.
134) Matsuura, Y., Stewart, M., Kawamoto, M., Kamiya, N., Saeki, K., Yasunaga, T. and Wakabayashi, T. (2000) Structural basis for the higher Ca^{2+}-activation of the regulated actin-activated myosin ATPase observed with *Dictyostelium*/*Tetrahymena* actin chimeras. J. Mol. Biol. **296**, 579–595.

(Received Apr. 16, 2015; accepted June 1, 2015)

Profile

Takeyuki Wakabayashi was born in 1941 in Osaka. He graduated from the Medical School at the University of Tokyo in 1965, and after spending his internship at the Hospital of the University of Tokyo in 1966, he received his Ph.D. from the Graduate School of the University of Tokyo in 1970. He continued his biochemical and biophysical research as an Exchange Fellow of the Royal Society and a short-term staff at the MRC Laboratory of Molecular Biology (Cambridge), as a research associate at the physics department of the University of Tokyo in 1973, and, since 1988, as a professor at the department of physics at the University of Tokyo, where he studied the structure of actin-tropomyosin-troponin filaments to establish the molecular mechanism of the Ca^{2+}-regulation of muscle contraction using electron cryo-microscopy. After retiring in 2001, he was appointed Professor Emeritus at the University of Tokyo and joined Teikyo University as a professor of biosciences to further study the regulatory mechanism of muscle contraction. He became the vice-president of the Biophysical Society of Japan in 1992–1993. He has also served as a member of the organizing committee of the Gordon Research Conference on Muscle Proteins in 1978, as an Advisory Editor and a member of Editorial Board of the Journal of Muscle Research and Cell Motility, as a member of Editorial Board of the Journal of Structural Biology, and an Associate Editor of Genes to Cells. He has been awarded the Seto Prize from the Japanese Society of Microscopy in 2003, and the Naito Foundation Merit Award for Advancement of Science from the Naito Foundation in 2001.